UCLouvain

École polytechnique de Louvain

Synthesis and characterization of solid electrolytes based on vitrimer-like ionically-conducting polymers

Authors : **Elina Nazmutdinova**
Supervisors : **Jean-François Gohy**
Readers : **Charles-André Fustin, Alexandru Vlad**
Academic year 2020–2021
Master [120] in Chemical and Materials Engineering

Acknowledgements

By this acknowledgment, I would like to express my deepest appreciation and gratitude to everyone who supported me and contributed to my thesis work.

To begin with I would first like to thank my supervisor, Professor Dr. Jean-François Gohy, who kindly accepted me to be a member of his research group and shared thoughts and his vision on the problems crucial for a bright future.

I would also like to thank my tutors, Dr. He Jia and Carla Barakat, for their valuable contribution to the development of the research methodology and continuous assistance throughout the experimental work carried out. Additionally, I would like to thank all the members of the research group for being so kind, helpful and ready to share some useful ideas.

As well, I would like to express my gratitude to the readers, Professors Dr. Charles-André Fustin and Dr. Alexandru Vlad, for investing their time to read the submitted work.

Last but not least, I could not imagine myself passing through this challenging path of FAME+ Master Degree without the great help, support and guidance of Igor Mikhaylov and other members of my family, and for sure, my friends.

Abstract

The discovery of highly conductive Li-ion solid electrolytes had a lot of advantageous consequences. Thus, all-solid-state Li-ion batteries have become a promising route towards improved safety and higher energy density compared to today's Li-ion batteries comprising liquid electrolytes. Nevertheless, limited Li-ion charge transport over the solid-solid electrode-electrolyte interface remains to be a great challenge towards high-performance all-solid-state batteries.

The following project proposes a novel solid polymer electrolyte design that may help to tackle the existing problems. The concept behind the development is in using the cohesive and deformable properties of dynamic covalent polymeric network driven by disulfide metathesis reactions at room temperature. This will be used to maintain the electrolyte-electrode contact interfaces improving the movement ability of the polymer network, thereby enhancing the ionic conductivity of the solid polymer electrolyte. As well as lowering the interface impedance and blocking the Li-metal dendrite penetration.

This opens up the possibility to safely apply Li-metal as a high-capacity anode, which in combination with a high Li-ion conductivity provides a strategy towards high-performance all-solid-state batteries.

Table of Contents

LIST OF FIGURES

LIST OF TABLES

LIST OF SCHEMES

LIST OF ABBREVIATIONS

ATR	Attenuated total reflection
CAN	Covalent adaptable network
CPE	Composite polymer electrolyte
DMAP	4-Dimethylaminopyridine
DSC	Differential scanning calorimetry
DTG	Derivative thermogravimetry
EIS	Electrochemical Impedance Spectroscopy
EV	Electric vehicle
FTIR	Fourier transform infrared
GPE	Gel polymer electrolyte
IL	Ionic liquids
LAB	Lead-acid battery
LB	Lithium battery
LIB	Lithium-ion battery
LIPB	Lithium-ion polymer battery
LMB	Lithium metal battery
MW	Molecular weight

OM	Optical microscopy
PEGDE	Poly(ethylene glycol) diglycidyl ether
PEO	Polyethylene oxide
PTFE	Polytetrafluoroethylene
RT	Room temperature
SEI	Solid electrolyte interface
SPE	Solid polymer electrolyte
SSB	Solid-state battery
TBP	Tributylphosphine
TGA	Thermogravimetric analysis
THF	Tetrahydrofuran

Chapter 1

Introduction

Nowadays our lives are hard to imagine without numerous useful devices which are taken for granted. Like: portable digital gadgets such as smartphones, smart watches, tablets, notebooks; very helpful in day-to-day life smart home appliances as cordless vacuums, electric teeth brushes and many others. Moreover, ones may live a dream or still working hard towards one to ride a cool e-scooter or e-bike or even drive a Tesla car to work every day. The following list should underline the astonishing dissemination of the applications employing lithium-ion batteries (LIBs). This is to highlight that these days it is hard to find someone in the developed or developing countries who has never heard about devices based on the technologies involving the use of lithium-ion batteries [1].

Technological development within the domain of alternative energy sources has been strongly pushed forward by the pursuit of sustainability [2]. Thus, internal combustion vehicles relying on the natural sources of oil and gas has been gradually substituted by hybrid vehicles or recently developed fully electric cars [3]. In addition, key players of automotive industry such as Swedish company Volvo have recently claimed to sell only fully electric cars by 2030 while General Motors Corporation declared to sell only EVs by 2035 [4]. Therefore based on the available data on the market shares the competent specialists from Bloomberg managed to predict the escalation of the global market of the

EVs to 60% in the nearest 20 years [5]. Hence, the ubiquitous electrification can pave the way for the 'net-zero' CO_2 emissions in road transport already by 2050 [5].

The average annual 7% increase of the energy density of LIBs [5] allowed scientists to consider LIBs as a promising technology for off-grid power supply systems [6] to ensure the homogeneity of the intrinsic intermittency of renewable energy sources with solar and wind power as outputs [7]. Consequently, this technology might provide reliable access to the electricity to the developing regions [1] which could be crucial for a quality living of people.

Collectively, an astonishing progress of the LIBs technology exploration is owing to billion investments in the research activity all over the world [1] from the governmental organizations and various alliances [8]. As seen in Figure 1-1 a lot of countries within the European continent are currently involved in the research and development process of the energy storage solutions in a form of LIBs [8]. The research establishments are daily challenging material science to jointly endeavor to push the limits of the energy storage technology for the better future of the world.

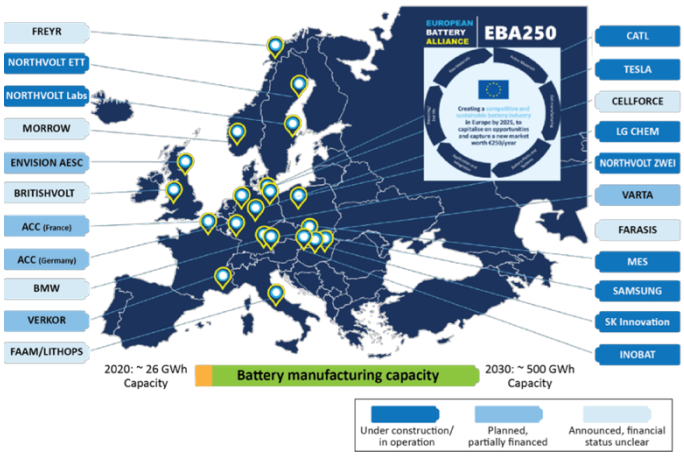

Figure 1-1 Planned LIB factories in Europe withing European Battery Alliance [8].

To understand the origins of such a high demand on LIBs' technology for various applications the list of which is constantly expanding and diversifying, a brief history of the technological revolution of electrochemical power storage systems should be introduced.

1.1 Batteries: definition

In general terms of electricity and electrochemistry, batteries are devices that convert electrochemical energy into electrical energy directly by undergoing an electrochemical oxidation-reduction reaction [9].

The main components constituting a single battery cell, the smallest unit of a device that is able to convert chemical energy to electric one, are positive and negative electrodes with a confined in between ionically conductive electrolyte [10]. Some additional components such as separators can be as well present in batteries to spatially isolate the electrodes within the system.

The main working principle shown in Figure 1-2 is based on the difference of chemical potentials of two electrodes of different nature which is, in turn, constitute an electromotive force of an electrochemical cell [11]. The electrodes should be connected via an external device creating an external electrical circuit to incite an electrochemical reaction. This reaction engenders the flow of the electrons from an electrode with more electronegative potential to the one with more positive potential [10]. Thus, ions move through the electrolyte to maintain the charge balance. In consequence, electrical energy can be trapped by an external circuit.

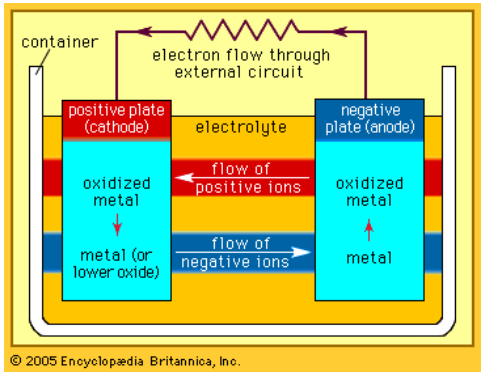

Figure 1-2 Basic components of an electrochemical cell [9].

Despite the fact that the described concept may sound to be inherently simple, the invention path was very thorny with plenty of challenges posed by limitations in the knowledge of material science. Nowadays many questions still remain unsolved. And some of them were attempted to be partially uncovered in future research.

1.2 Technical characteristics

Performance of different batteries can be described via several technical characteristics [12] which are as follows:

- Theoretical capacity, C: the number of charges that a battery can deliver from a fully-charged state to a state when battery is discharged. Measured in mAh/g. Determined via the number of electrons n injected or removed during cycling, and the molecular weight MW of the insertion material as follows:

$$C = \frac{nF}{3.6 * MW}. \tag{1-1}$$

Hereby, F stands for Faraday constant, and 3.6 is conversion factor for unit homogenization (coulombs and milliampere hours (mAh)).

- Energy, E: the total energy stored in or discharged from a battery. It corresponds to an integral of its voltage (V) with respect to its capacity C. Measured in Wh and calculated as follows:

$$E = \int V(C)dC. \tag{1-2}$$

- Energy density: amount of energy stored by a battery with respect to its mass (gravimetric) or volume (volumetric). Therefore, measured in Wh/kg or Wh/L.
- Power: the energy a battery can deliver per time unit. Quantifies the amount of current flowing at a given potential.

It is worth to mention that all the above-mentioned parameters are strongly dependent on the chemistry of the system with all its constituents.

1.3 Technology through ages

Once Gordon Moore predicted that every 2 years memory capacity of microelectronic devices was going to be doubled [13]. The law proposed by Moore is applicable to rapidly developing microelectronics industry which is pushing all the limits and boundaries of material science and engineering even reaching More than Moore state (when the miniaturization goes along with the increase of the performance).

You might think how it is linked to batteries technology being discussed here. Indeed, there is no direct link, but the fact introduced can help underline and highlight the complexity of the batteries' technology development path.

Thus, throughout the ages from the moment when lead-acid batteries (LABs) were considered to be a technology of choice for energy storage (in the 1860s) till the time when LIBs were first commercialized in 1991 by Sony, the stored energy increased only by a factor of 5 being $\approx 180\ Wh/kg$ at an average voltage of $3{,}8\ V$ [14].

Before deepening into the history of various batteries systems with different chemistries, it is the right time to introduce the notion of primary and secondary batteries. By convention, it was decided to call rechargeable batteries suitable for multiple time use as secondary ones, while primary batteries cannot be recharged and therefore suitable only for a single-use until the voltage is too low to fulfill the function to power a device [14].

1.3.1 Primary batteries development

Now let's return back to the moment when it all started to deliberate upon the evolution of the batteries. Hence, the first time when a battery was described was in 1800 and it was done by the Italian professor Alessandro Volta [15]. That time an electrochemical unit consisted of metal disks of different chemistries – silver or copper and zinc ones (Ag or Cu and Zn) separated by a piece of cloth soaked in an alkaline solution of sodium chloride ($NaCl$) in a form of the layered stack in a pile [16]. This invention was attributed to a class of primary batteries as the reported system could not be recharged by any means. The so-called battery presented by Volta produced an electric current through the connected ends of the pile stack with the $0{,}65\ V$ of electromotive force [17].

The discovery of Volta had a tremendous impact on the evolution of electrochemistry and boosted the further development of other batteries based on various chemistries. Consequently, in 1865 the French engineer Leclanché developed the first manganese cell which became widely used in telegraphy, signaling, and electric bells application [10]. The Leclanché cell was composed of a mixed manganese dioxide – carbon cathode ($MgO_2 - C$), a zinc anode (Zn) and an aqueous solution of ammonium chloride (NH_4Cl) or its mixture with zinc chloride ($ZnCl_2$) playing a role of electrolyte. A great success on the market resulted from the fact that the voltage of $1{,}4 - 1{,}5\ V$ provided by the cell was sufficient to fulfill the function of powering devices used in the 1860s.

Already at that time, one of the main disadvantages of the applied technology with liquid electrolytes was detected: the cells were not reliable because of the spillage and leakages. That is why the forerunner technology introduced by Leclanché was adapted in this regard and the 'dry cell' concept was proposed by the German scientist Carl Gassner in 1886 [18]. A standard cell comprised a carbon cathode, a zinc anode, and paste-like ammonium chloride thickened by additional chemicals. Various plasticizers were tested with starch and flour being the first jellifying agents tested, but the most performant one turned out to be gypsum plaster known as Plaster of Paris ($CuSO_4 \cdot \frac{1}{2} H_2O$). A small spoiler: the concept of electrolyte thickening has been adopted in the most recent technologies for LIBs in a form of gel-like polymer electrolytes and very promising results had been already obtained for numerous systems [19], but we will return to this in the upcoming sections.

As time passed, a new class of batteries emerged when an acidic aqueous ammonium solution in the Leclanché cell was substituted by a concentrated potassium

hydroxide (KOH) electrolyte solution. This was of the origin for the name of the new batteries class – alkaline batteries. Likewise Gassner cells, latter were thickened by gelling agents such as sodium polyacrylate or polyacrylic acid [20]. The use of the new electrolyte chemistry allowed to enhance the performance of the batteries in terms of batteries' capacity and discharge time. By now alkaline batteries have still remained to be very handy for powering so-called low-power household devices.

But the peak performance of primary batteries was reached when the first lithium metal batteries (LMBs) of 3 V with lithium metal (Li) as an anode were introduced and commercialized in the 1970s [10]. Nevertheless, the primary LMBs technology, being still widely used, doesn't allow to recharge batteries. That is why a new concept based on reversibility of electrochemical reactions and intercalation chemistry was applied in order to induce rechargeability into the system and make the best use of lithium-ion batteries [21].

1.3.2 Secondary batteries development

Since the introduction of the first Volta battery prototype, battery technology has become one of the most widely exploited. Thereby a high demand from numerous fields of applications where the batteries can be employed promoted further development and advancement in the understanding of the existing processes. Moreover, a great number of evolving applications required a rechargeable multi-use power source. This gave a rise to the development of secondary batteries.

A good visual representation of the secondary batteries technology development of over time is shown in Figure 1-3 [14]:

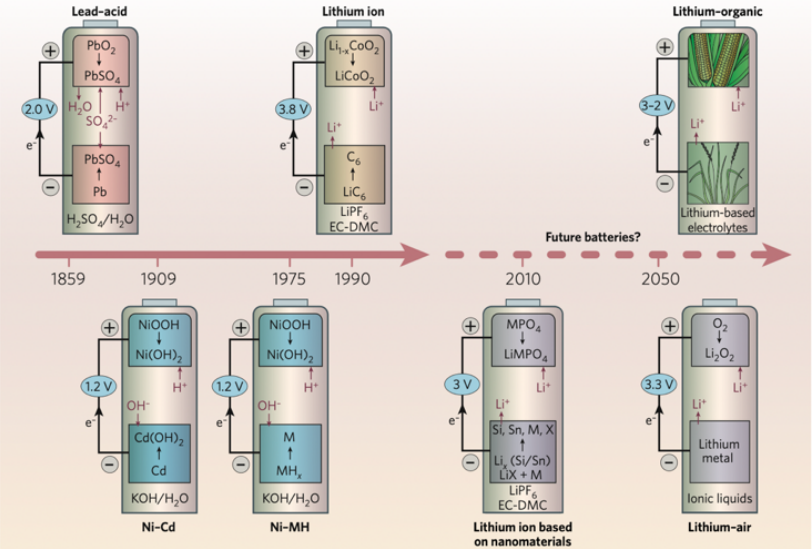

Figure 1-3 Secondary batteries chemistry over the years [14].

The oldest type of secondary battery invented by the French physicist in 1859 was the lead-acid one [22]. A system provided 2 V of electromotive force and constituted of a lead metal anode (Pb), a lead peroxide cathode (PbO_2), and a weak sulfuric acid (H_2SO_4) as an electrolyte. The rechargeability of the system was assured by the reversible electrolysis reaction. Thus, while discharging lead (IV) – oxide in sulfuric acid is reduced to lead (II) – sulfate ($PbSO_4$) at the positive electrode, and metallic lead is oxidized to lead (II) – sulfate at the negative electrode. Whereas when the cell is fully discharged, both the positive and the negative electrodes are converted to lead sulfate with electrolyte dilution by the by-product of the electrochemical reaction – water.

Overall, lead-acid batteries being the oldest secondary batteries they are still in use, mainly in cars. This is possible thanks to numerous recognized merits. Therefore, the LABs' technology is being very mature, batteries themselves are relatively cheap, reliable, and can be manufactured in different sizes. Moreover, the well-developed lead-acid

batteries recycling technology enables to recycle of up to 98% of the used items [23]. But along with it, some critical drawbacks don't allow LABs to be used in high-tech EVs. This is to be low energy to volume and energy to weight ratios with an energy density of approximately $30 - 50 Wh/kg$, relatively short life (up to 1000 cycles) [24]. The mentioned disadvantages didn't go along with the concept of lightweight modern electric cars for daily use where the massive pack of LABs would decrease the EVs performance. This was a reason for the technology to be revised.

Consequently, the nickel-cadmium ($Ni - Cd$) batteries were invented by Waldemar Jungner in 1899 [25]. Conventional nickel-cadmium battery consists of cadmium anode (Cd) which is oxidized to cadmium hydroxide ($Cd(OH)_2$) during discharge and nickel oxide hydroxide cathode ($NiOOH$) reduced to nickel hydroxide ($Ni(OH)_2$), with potassium hydroxide as an electrolyte (KOH) [26].

Unfortunately, the progress of this technology was hindered by processing limitations. That is why only after the 1930s when deposition and sealing techniques did advance, the nickel-cadmium batteries had become a favored technology of use as a reliable uninterruptable power supply [25]. $Ni - Cd$ batteries were more robust compared to the existing at that time LABs having a higher energy density of $50 - 75\ Wh/kg$ and a longer life (up to 2500 cycles) with $1{,}2\ V$ of electromotive force [24].

Furthermore, $Ni - Cd$ batteries were able to serve at higher temperatures and required less maintenance than existing LABs. However, the increased consciousness in environmental aspects of life in the 2000s followed by a change of the local regulations concerning the use of toxic cadmium led to a drop in sales of $Ni - Cd$ batteries.

In addition to this, $Ni - Cd$ batteries possess a very peculiar feature called the memory effect. Generally, the memory effect is attributed to the loss of battery capacity when being recharged after being not fully discharged. This makes $Ni - Cd$ batteries to be unsuitable for use in variable renewable energy sources technologies such as solar and wind power supply since those energy sources are non-dispatchable and may include forecasting errors. Therefore, the use of $Ni - Cd$ batteries most of the time is economically unfeasible due to the high risk of problems arising from the memory effect.

Above all, the operation of the earlier discussed lead-acid and nickel-cadmium battery systems is claimed to be accompanied by liquid electrolyte consumption in the chemistry of the batteries [14]. This phenomenon decreases the content of the energy stored by a battery cell which is one of the most crucial measures of battery efficiency. No wonder why the further technologies of newer battery types did supersede the existing ones. As a consequence, a new concept based on intercalation chemistry was introduced into batteries' technology.

Thus, a new nickel-metal hydride ($Ni - MH$) system allowed to ensure electrolyte conservation. This was achieved through the reversible insertion to and extraction of protons H^+ from electrode materials with the attendant addition or removal of electrons. Nickel-metal hydride batteries are similar to the nickel-cadmium ones, but outlawed for many applications cadmium anode is replaced by metal hydride one [26].

One of the main advantages of $Ni - MH$ batteries is a high power density of about $1000\ kW/kg$ which quantifies the ability to deliver stored energy per unit time. Albeit, the nickel-based technologies are very promising, especially $Ni - MH$ as being more

environmentally friendly, they remain to be very expensive due to the continuously increasing price of nickel [25].

Altogether, lead-acid, nickel-cadmium and nickel-metal hydride systems are still present in various markets. But a strong tendency for their replacement can be seen [27]. Additionally, the series of scientific breakthroughs in the late 1960s originated the increase of the demand for portable energy sources for application in implantable medical devices, for developing electronic market, and for very special military applications [16].

Eventually, the lithium metal secondary batteries came to light in the late 1890s. A system was built up from a lithium metal (Li) anode and a molybdenum or titanium disulfide (MoS_2 or TiS_2) cathode with an electrolyte in a form of lithium salt dissolved in an organic solvent [28]. Further cathode material was replaced by metal oxide (as magnesium oxide – MnO_2). Nevertheless, the introduced technology didn't meet the requirements for safety due to the high reactivity of the metallic lithium anode. Thus, a short-circuiting could occur as a consequence of the electroplating of the lithium from the electrolyte on the lithium-metal anode during charging. This tremendously destabilized the surface properties leading to a growth of the dendrites which were the cause of the cell failure via short-circuiting when dendrites pierced the opposite electrode. In the worst case, this could result in thermal runaway and even explosions [29].

That is why lithium-carbon intercalation compounds were considered as a good solution for this problem in lithium-ion batteries [12]. And hence, tackled by this way challenge found its use in the modern secondary batteries [1]. Therefore, the end of the

1990s was marked by large-scale use of the lithium-ion system technology with a displacement of the other ones [27].

In accordance with the history of the development detailed above the comparative chart with respect to the batteries' performance is presented in Figure 1-4 [30]. So that one may conclude that the lithium-ion batteries which are dominating today's market are the technology of choice for the most recent and future high-tech applications being the most efficient among others. Moreover, the LIBs systems are constantly evolving to satisfy the most all safety aspects. Based on these considerations, plastic LIBs (PLiON in the below chart) were introduced to the world [31].

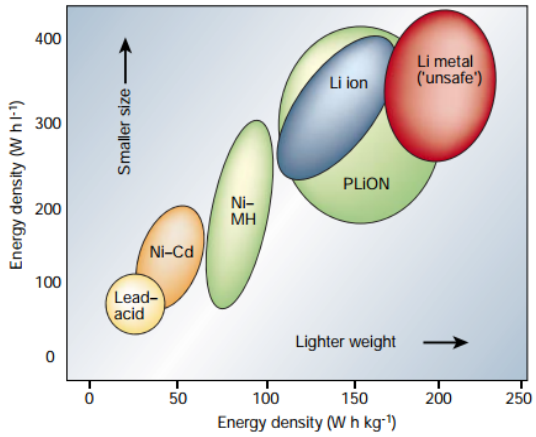

Figure 1-4 Energy density of different secondary batteries [30].

As an outlook, further development of the batteries' chemistries can be expected. Currently, numerous countries target gradual electrification to reduce the amount of greenhouse gases emissions and in the future to become fully independent from non-renewable energy sources. This can be achieved through advancing the technology: both

in forging ahead performance of the batteries challenging new chemistries as well as making attempts to increase eco-friendliness of the system.

1.4 Lithium-ion batteries

LIBs possess a unique combination of the properties essential for power supply application such as high specific energy and power same time having relatively low discharge rates [1]. Thus, understanding the working principle of the batteries is of great importance in order to deepen further into more advanced topics and elaborate on the various system components and their chemistries.

1.4.1 Working principle

Lithium, being the lightest metal, has the lowest reduction potential [10]. This enables to generate working voltages of more than $3\,V$. Also, lithium-ion has the smallest ionic radius from any single charged ion which translates to its high ionic mobility [32]. There is the reason for LIBs having the high volumetric and gravimetric capacity and power density.

LIBs can be attributed to a class of secondary batteries signifying the possibility of an electrochemical cell undergo several cycles of charge and discharge. This has become possible to sequential intercalation and deintercalation of lithium ions into electrode materials [12]. It is to say that the lithium ions are shuttling back and forth between the electrodes during the working cycles of the battery. The first commercially successful system which was implemented into numerous applications was presented by Sony in 1991 [33]. It was comprised of a metal oxide cathode and a graphite anode. For such systems

electrochemical reactions can be represented accordingly with Scheme 1.4-1 Electrochemical reactions in conventional LIBs.:

Positive electrode $LiMO_2 \underset{discharge}{\overset{charge}{\rightleftharpoons}} Li_{1-x}MO_2 + x\,Li^+ + xe^-$

Negative electrode $6C + x\,Li^+ + xe^- \underset{discharge}{\overset{charge}{\rightleftharpoons}} Li_xC_6$

$$LiMO_2 + 6C \underset{discharge}{\overset{charge}{\rightleftharpoons}} Li_xC_6 + Li_{1-x}MO_2$$

Scheme 1.4-1 Electrochemical reactions in conventional LIBs.

The general working principle during charge and discharge cycles can be represented as shown in Figure 1-5 (below):

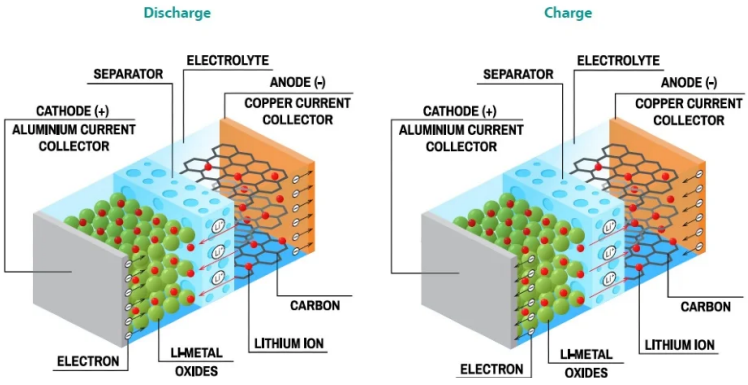

Figure 1-5 LIB during charge/discharge cycles [34].

Therefore, discharge corresponds to the intercalation of the lithium-ion into available sites in the cathode material. This is driven by a spontaneous redox reaction during which the reduction of electroactive species of a cathode material occurring at the surface of a positive electrode. While the flow of electrons from a negatively charged to a positive electrode through an external circuit maintains the electroneutrality of the system.

During recharge of the battery, the externally connected power source reverses the flows. Hence, reverse processes occur. Electrons flow back to the negative electrode, then metal M^{x+} is oxidized and lithium ions deintercalate from the positive electrode and intercalate to the negative one. A summary of the processes taking place during work cycles is presented below in Table 1-1:

Table 1-1 Summary of the direction of ion and electron transport at both electrodes of an intercalation-based battery during working cycles [12].

	Charging	**Discharging**	
Positive electrode	Intercalation Reduction	Deintercalation Oxidation	Ionic process Electronic process
Negative electrode	Deintercalation Oxidation	Intercalation Reduction	Ionic process Electronic process

To conclude, LIBs based on the described above working principle represents the state of the art of the current and future electrochemical technology for energy storage.

1.4.2 Constituents

After discussing the development of the batteries technology and, in particular, lithium-ion batteries systems it has become obvious that LIBs are very versatile systems [35]. Consequently, the performance of LIBs is a function of the properties of all constituting components. In other words, the choice of the material determines the properties of the cell. And as it was earlier mentioned, LIBs are composed of positive and negative electrodes, electrolytes and separators if needed. The way of finding proper materials to fulfill the function assuring the safety aspects was and remains to be very challenging.

1.4.2.1 Electrodes

As regards electrodes, the function of electrodes is to reversibly host and release lithium ions while maintaining their initial crystal structure without collapsing of the lattice when lithium ions are deintercalated and at the same time balancing the positive charge when ions are inserted inside the lattice [30]. It means that electrodes should be reliable in terms of both assuring electronic stability and stability of the crystal structure without any side reactions or phase transformations. This is to guarantee a good cycle life with minimal capacity loss. Cycle life characterizes the number of charge/discharge cycles a battery can undergo till fading of the capacity to 80% from the initial one. Along with it, good electronic and ionic conductivity of electrode materials are required.

Thus, in 1980 astonishing results were obtained with the use of transition metal oxide of lithium and cobalt ($LiCoO_2$ – LCO) cathode disclosed by Goodenough [36] who was, by the way, awarded with Nobel Prize in 2019. This commercially successful inventory pathed the way for further developments and sequences of newly discovered systems. It might also be noted hereby that current commercial batteries are named by the lithium-ion donator material i.e., the cathode.

Concerning anode, the predominant technology is graphite-based materials as it allows the lithium intercalation between the graphene planes providing good 2D mechanical stability, sufficient electrical conductivity, and Li ions transport [32]. That is why graphite being abundant and hence cheap is widely used in commercial LIBs. But some other non-carbonaceous anode materials are known and used. For instance, lithium

titanate $Li_4Ti_5O_{12}$ – LTO which is a safe alternative of lithium anode for high-power batteries having a higher lithiation potential than the one of graphite [35].

In brief, the most common and widely used electrode materials with their technical characteristics are gathered in Table 1-2 below:

Table 1-2 Rechargeable Li-ion battery intercalation electrode materials [12].

	Material	Average voltage (V vs. Li)	Practical capacity (mAh/g)
Cathodes	$LiCoO_2$ (LCO)	~3.9	140
	$LiMn_2O_4$ (LMO)	~4.1	120
	$LiFePO_4$ (LFP)	~3.45	160
	$LiNi_{1/3}Mn_{1/3}Co_{1/3}O_2$ (NMC)	~3.8	200
	$LiNi_{0.8}Co_{0.15}Al_{0.05}O_2$ (NCA)	~3.8	200
Anodes	Graphite (LiC_6)	~0.1	360
	$Li_4Ti_5O_{12}$	~1.5	175

As it was earlier underlined, the choice of materials determines the performance metrics of the system. So that the system efficiency can be tuned in accordance with different working conditions fitting the best-expected properties same time assuring safety and minimizing the costs. Material selection should include ecological considerations as well. Likewise, according to the thermal stability of the constituents' chemistries, the thermal stability of a battery unit can be adjusted.

Based on the discussed, Figure 1-6 above might be considered as a hint for material selection when thinking about battery system composition.

Figure 1-6 Cathode materials for commercial Li-ion batteries [1].

Nonetheless, as for every engineering problem not only chemistry determines the performance but the manufacturing process as well [37]. And for electrode materials, the impact is very pronounced. As known, all the compounds suitable for applications as positive electrodes (presented in Table 1-2) possess higher impedance comparatively to metallic lithium and thus have lower conductivities. One of the ways to overcome this problem was to refine lithium-based compounds and blend them with a conductive material, such as conductive carbon [1]. To facilitate the shaping step additional elements are usually required: a solvent (e.g., n-methyl-2-pyrrolidone – NMP) and a binder (e.g., polyvinylidene fluoride – PVDF). Anode material preparation proceeds analogously. The electrode slurry (mixture in a form of the paste containing active material and additional components) should be pasted onto the surface of aluminum (for cathodes) and copper (for anodes) foils acting as battery cell terminals.

Overall, manufactured electrodes should be dense enough to assure mechanical integrity, but same time be permeable to ions. The current state-of-the-art industrial technique of electrodes processing is the slot-die coating when the slurry is dosed onto the terminal foils through a precise coating head [37]. The most commonly used equipment for coating at the lab scale is the so-called doctor blade which allows controlling the thickness of the deposited layer of the paste. The coating step is followed by the drying step to extract the solvent and calendaring to compress down the material till the required thickness and density extent. As well, one of the recently developing techniques that allows to design a desired shape of channels for ion conduction is 3D printing [38].

A general trend of the reduction of the amounts of solvent used can be noticed. As most of the time, organic solvents are highly flammable and not eco-friendly. Furthermore, the more solvent is used the more energy is required for its extraction, not saying that it as well increases the chances to have some solvent remained in the closed pores of the electrode structure. Ideally, fully dry processing techniques are to be used.

1.4.2.2 Electrolytes

By definition, an electrolyte should be simultaneously an electrical insulator and an ionic conductor [12]. It is to permit ionic transport whilst disallowing cell short-circuiting.

The role of the electrolyte was anticipated by Volta himself in his works in the late 1700s. He noted that the electric current in the pile he constructed was not totally free. It was hindered and sequentially delayed by the electrolyte layers [16]. Already at that time, one of the main challenges had been pointed out. This is to say that electrolytes bear a critical role in directly influencing the electrochemical behavior of the battery.

Electrolytes used in LIBs can be classified into four main groups which are liquid, polymer, inorganic, and composite. Careful choice of electrolytes can guarantee an optimized safe working life of the battery. So, let's go through the main types of electrolytes in more detail.

Liquid electrolytes

The majority of the present commercially available LIBs employ an organic Li-ion conducting solution as an electrolyte. A well-established approach is based on the use of the mixture of several chemicals carrying particular functions [35]. Therefore, an electrolyte is composed of lithium salt, organic solvents, and additives. The more components are within the systems, the more degrees of freedom are. This increases the latitude of the case complexity as every constituting element is burdened with a list of numerous constraints to fulfill the function properly.

Organic solvents within the electrolyte multi-component system ideally should have a high dielectric constant to favor the dissociation of lithium salts, low viscosity to assure fast movement of ions, low volatility translating to a high boiling point to ensure safety [39]. Additionally, the solvent should not be reactive towards the materials of electrodes (both active and supporting materials composing the electrodes). The solvents should have low toxicity not to cause problems if leakages occur. As well toxicity is crucial in terms of disposal or recycling considerations. Those conditions should be necessarily satisfied to guarantee a proper and safe work of the battery.

Current technology employs the use of mixtures of carbonate solvents: cyclic (e.g., ethylene carbonate – EC) and linear (e.g., dimethyl carbonate – DMC, ethyl methyl

carbonate, diethyl carbonate – DEC) ones. The two types of solvent are mixed to balance the properties. Therefore, EC which has low volatility and exhibits a high dielectric constant enabling effective dissolution of lithium salt, has a rather high viscosity dumping the transport properties. So that linear carbonates possessing low viscosity can dilute a thick EC medium. This leads to an increase in the fluidity of the system and hence ion transport is facilitated.

The most basic salt used in commercial LIBs is lithium hexafluorophosphate – $LiPF_6$. Besides its high ionic conduction, it shows a wide electrochemical stability window and good ability toward the formation of the solid-electrolyte interface in carbonate organic solvents solution. The latter is important meaning that corrosion of current collectors can be avoided. The main disadvantage of the $LiPF_6$ is its poor thermal stability which leads to the formation of very active hydrogen fluoride – HF upon decomposition. This can lead to the dissolution of the transition metal ions in the cathode material.

The additives are brought up into the system to enhance the safety not affecting its electrochemical performance. Most of the time, flame-retardants or solvents with a high flash point can be used for this purpose. So that, vinylene carbonate – VC and fluoroethylene carbonate – FEC are the most common ones. As well, the use of EC as additive within the system is proceeding with the formation of a stable solid-electrolyte interface with the electrolyte solution, meaning that proper reversible intercalation of lithium cations for thousands of cycles can be assured

All the main components discussed above with their chemical structures are represented in Figure 1-7 below:

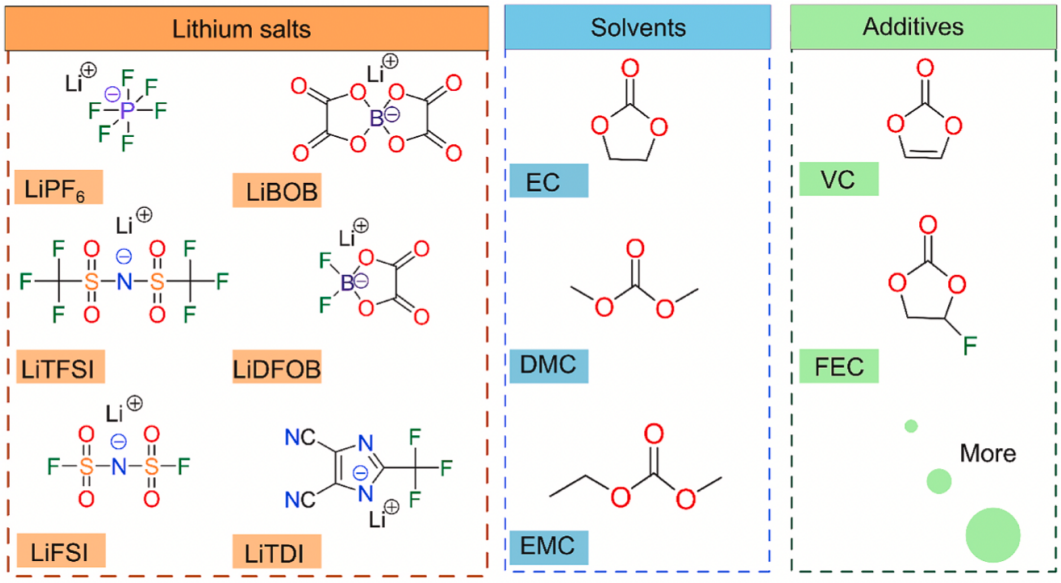

Figure 1-7 Chemical structures of the main components constituting the state-of-the-art liquid LIBs [35].

Despite the fact that the technology described earlier is widely used in commercial LIBs, a lot of safety issues were reported [40]. The conventional LIBs are designed to be used at the operation temperatures up to 40°C and overpassing this threshold may lead to irreversible consequences caused by the decomposition of the systems. Batteries being a very complex system can have various mechanisms of failure, but hereby thermal abuse can be considered as the most crucial one [40]. Therefore, non-controllable self-heating causing by thermal runaway in the battery with liquid electrolyte can lead to combustion or even explosion of the battery.

To conclude, in spite of the fact that liquid electrolytes are of great safety concern, they remain to be widely used due to the best ionic conductivity. This safety problem was attempted to be tackled through the use of other compounds.

Ionic liquids are one of them. Basically, ionic liquids are salts that have their melting point below room temperature. Due to the high asymmetry of the ions, ionic liquids stay in a molten state at room temperature [41]. When those compounds are used as electrolytes it enhances the safety of the system as ionic liquids have a low vapor pressure. Nevertheless, it originates other problems which prevent the wide implementation of this technology at a large commercial scale. Their viscosity is relatively high.

Based on the same safety considerations, a lot of attempts were endeavored to find other more promising and reliable organic solvents. Thus, organosilicon-containing electrolytes and various fluorinated and phosphonated electrolytes showed good results in terms of low flammability and very delayed ignition [42]. Although the safety can be a bit improved, solid electrolytes are aimed as they not only improve safety but are more beneficial from an engineering point of view to shorten the number of operations during manufacturing and to engender useful mechanical properties.

Polymer electrolytes

Even though LIBs with liquid electrolytes are still widely used nowadays they have a lot of safety issues. The research interest driven by the will to battle these challenges led to a list of numerous academic breakthroughs. So that now, two main classes of polymer electrolytes can be distinguished: gel polymer electrolytes (GPE) for quasi-solid batteries and dry solid polymer electrolytes (SPE) for solid-state batteries [43].

Within those big classes, many types of systems can be recognized and the simplified classification is presented below in Figure 1-8:

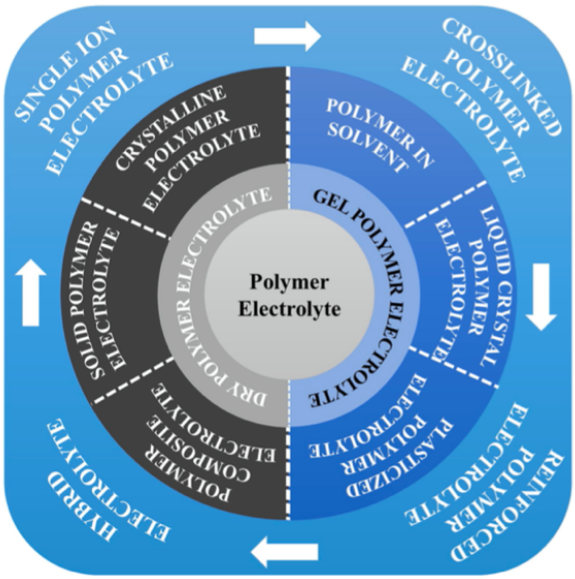

Figure 1-8 Simplified classification of commonly investigated polymer electrolyte systems [44].

Gel-polymer electrolytes represent polymer matrix with confined in it solvent and lithium salt. One of the main factors which determines the conductivity is the strength of the polymer-solvent interaction being a measure of the system stability. A great advantage of gel-polymer-based electrolyte systems is their improved mechanical characteristics with a range of conductivities approaching the ones of systems with liquid electrolytes. But still the use of solvents presents some safety concerns. That is why currently, a common trend towards the use of true solid electrolytes is observed. In accordance with predictions, this approach will most probably dominate the future market.

A history-changing breakthrough was made in 1873 when the formation of alkali metal-ion conductive complexes based on polyethylene oxide (PEO) polymer matrix was reported. Meaning that polymer can act as a ‘solvent’ and conductive medium for alkali metal salts [43]. Due to coulombic interaction PEO segments coordinated to the lithium

ions favor the dissociation of the lithium salt. And in a presence of an external electric field, alkali-metal cations migrate from one coordination center to another and thus showing conductivity. This concept was soon applied in lithium-based batteries with solid-polymer electrolytes. But the shown conductivity was not acceptable as the cells were to be used at RT. This pushed research efforts on a deeper understanding of the conductivity mechanisms.

Hence, the investigation showed that the ionic motion occurs both through the migration of the cation species due to micro-Brownian segmental motion of the PEO backbone (takes place in amorphous regions) and through the ion hopping from site to site (in crystalline regions). Conventional mechanisms are shown in Figure 1-9.

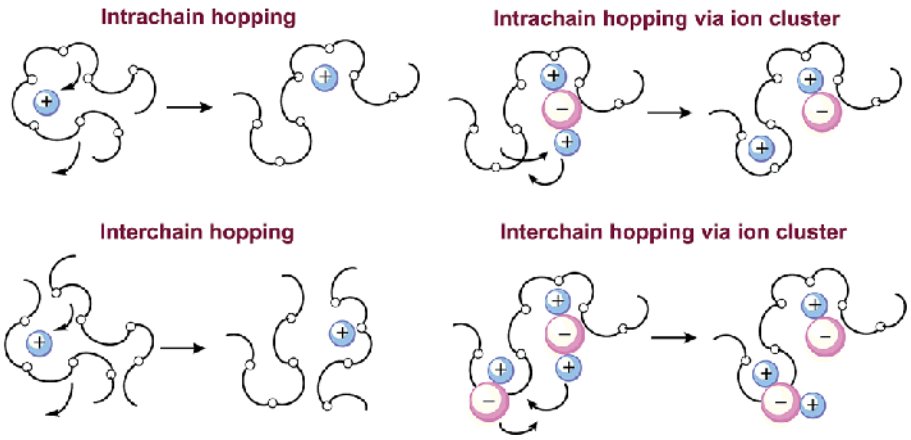

Figure 1-9 Mechanism of ion transport in PEO [45].

The reached ionic conductivity in crystalline regions was of the range $\leq 10^{-6}\ S\ cm^{-1}$ and $> 10^{-4}\ S\ cm^{-1}$ in amorphous ones. That is why scientists came up with the idea to tune PEO crystallinity to promote higher conduction in amorphous regions. So that cross-linking and use of branched PEO derivatives were found to be a solution with reaching conductivity of the range $\sim 10^{-4}\ S\ cm^{-1}$ at RT for some particular systems.

Because PEO was the first polymer investigated the majority of the studies refer to the use of PEO and its derivatives as SPE for LIBs. In fact, not only PEO-based chemistries exist and can be applied in LIBs. Therefore, polycarbonate-, polynitril-, polyester-, polysioxane- based SPE are currently under investigation [43, 46]. A recent discovery of a new type of SPEs based on charge-transfer complexes can potentially dramatically change the LIBs technology [47]. The conductivity of SPEs that were reached was of the range of liquid ones $10^{-3} - 10^{-4}\ S\ cm^{-1}$ at RT. Nevertheless, a lot of questions including the exact mechanism of lithium transfer remain open.

Overall, SPEs helped to solve many issues attributed to the use of liquid electrolytes and thus, increased the safety of the LIB systems. Moreover, they allowed inducing flexibility and improved mechanical properties of the batteries by this opening doors for new applications of LIBs. Additionally, solid polymer electrolytes show lithium dendrite growth suppressing, this makes them suitable for use with high-capacity Li-metal anodes [43, 48, 49]. This potentially enables the manufacturing of products with outstanding electrochemical performance and safety.

Inorganic electrolytes

Based on the considerations described above, one may think that if using inorganic solid electrolytes in lithium solid-state batteries all problems inherent to other types of electrolytes could be solved.

Indeed, the use of ceramic electrolytes significantly increases the safety of the system, but same time introduces other constraints into the system mainly ascribed to the list of very particular intrinsic mechanical properties of this material family.

The most common classes are oxides, phosphates, and sulfides [50]. All of them show outstanding chemical and thermal stability having a moderate conductivity at RT. It is worth mentioning that the conduction mechanism strongly depends on the lattice type and the available sites for lithium-ions hopping [51]. Those migration mechanisms shown in Figure 1-10 can be either through vacancies, direct interstitials, and correlated (interstitialcies) ones. Moreover, conduction might proceed through various mechanisms simultaneously involving single or multiple sites. Additionally, it was proved that ion-conduction in ceramic-based electrolytes happens at different scales: from atomic to device one, which brings up additional complexity to the fundamental understanding of the system.

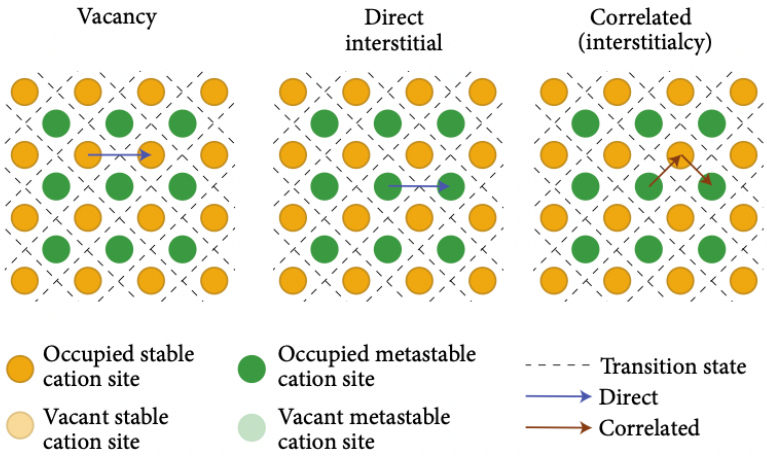

Figure 1-10 Cation migration mechanisms [51].

Unfortunately, this type of electrolyte is facing numerous challenges which stops the wide spreading of this technology at a large scale. Mainly it is the intrinsic brittleness of ceramic materials which makes them be fragile and not flexible [51]. Furthermore, the formed interfaces with electrodes are very unstable often leading to contact loss.

Composite electrolytes

In the material selection approach developed by M. Ashby hybrid solutions can be considered as a middle ground to get the best from several material classes at once [52]. So was done by numerous of scientist used composite systems for LIBs application [53-55]. This allowed reaching good electrochemical performance while having safe and mechanically reliable systems. As in every hybrid system, the ratio between the components dictates which properties are to be more pronounced.

Hereby, within the scope of this thesis, the development of this kind of system was not aimed. That is why a more detailed description would be omitted.

1.4.2.3 Separators

Separators were not usually paid much attention to throughout the history of battery technology development. Nevertheless, separators play a key role, especially in technologies with not very reliable electrolytes, such as liquid ones. Thus, a function of the separator is to prevent the shorting of the cell through direct or indirect electrode-electrode contact while allowing the transportation of the moving lithium ions [56].

The ionic conductivity of separators can be an intrinsic property of the electrodes separating material. For instance, this is a case of earlier described solid electrolytes (both inorganic and polymer ones) which basically additionally carry a function of separators. Otherwise, ionic conductivity might be artificially induced by soaking separator materials in ionically conductive electrolytes. In that case, the separator material should show minimal ionic resistance not to decrease the electrical performance of the cell.

Currently, the most commonly used separators in commercially available LIBs with liquid electrolytes are polyethylene and polypropylene in a form of microporous membranes [56]. Not only do they bear expected functionality, but they exhibit additional safety effects, so-called “shutdown” [1]. It can be observed when the cell excessively heats up, the separator simply melts blocking the ionic flow. This helps to avoid the worse consequences of thermal runaway. But as discussed in the previous sections, based on safety concerns a general trend toward the development and use of all-solid-state batteries can be observed.

1.5 Vitrimers

A novel class of polymers that was recently discovered blurred a border between conventional thermoset and thermoplastic polymer materials. Thus, a promising chemical strategy when plasticity was introduced into a cross-linked polymer network gave a rise to the development of vitrimers [57]. The vitrimer behavior is characterized by a gradual viscosity decrease with the increasing temperature.

Vitrimers are polymer materials with dynamic cross-links. The dynamic network exists thanks to the presence of exchangeable bonds known as covalent adaptable networks (CAN) of associative type. A simplified exchange concept standing behind so-called vitrimers is presented in Scheme 1.5-1:

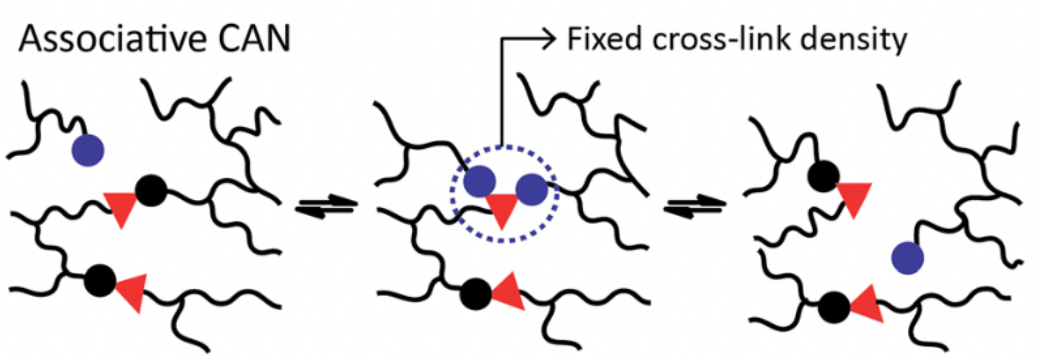

Scheme 1.5-1 Schematic representation of the associative CAN [57].

Associative exchange in between the bonds is characterized by the fixed cross-linked density. This can be explained by the fact that in vitrimers, an existing initial cross-link can be broken only if a new covalent bond can be formed in a new place. It means that the formed network is permanent and dynamic at the same time.

The explained phenomenon induces very particular features to this type of material. The dynamic network can change its topology upon stimuli. Therefore, vitrimers behave like viscoelastic liquids at elevated temperatures when the associative exchange reactions are triggered by an increase in temperature. While acting more like thermosets when cooled down. Hence, at ambient temperatures, these materials are very robust in terms of mechanical properties.

Vitrimers can be considered to be sustainable materials because of their unique properties of changing their topology [58]. They are malleable and thus, can be potentially reshaped or reprocessed. Which is, by the way, impossible for conventional thermosets and originates a lot of concerns about thermosets recyclability. Additionally, these types of materials have successfully been shown to possess self-healable properties [59, 60].

Chapter 2

Aim and context of this research

2.1 Research background

The previous chapter extensively covered the state of the art of the today's energy storage technology. Thus, LIBs being widely used and seen as ideal candidates for many applications relied on rechargeable power sources should fulfill the highest safety standards in order to be considered for further implementation in a number of new high-tech devices. Among all the possible batteries configurations, the highest safety with acceptable performance can be assured by solid polymer electrolytes.

Hence, solid polymer electrolytes (SPE) are considered to be the safest technology for LIBs [61]. Nevertheless, one of the main challenges towards the high performance of all-solid-state batteries is limited Li-ion charge transport over the solid-solid electrode-electrolyte interface (SEI). Some possible contributions to this interface resistance include loss of electrode-electrolyte contacts as a result of the electrode volumetric changes, interface reactions, and space charge layers driven by the difference in electrode and electrolyte electrochemical potential.

The most recent researches proved that the quality of the ion transport through SEI can be improved via using self-healable polymer materials as electrolytes and components for electrodes [43, 62].

This has given rise to a new class of batteries known as smart batteries. The self-healing properties induce self-repairing of internal mechanical damages without batteries' failure. Furthermore, these properties allowed using high-capacity Li-metal anodes which was completely unattainable for secondary Li-metal batteries with liquid electrolytes because of lithium dendrites growth. Generally, polymer network in SPEs hinders the dendrites growth. However, the majority of available SPEs suffers from unstable SEI resulting in increased resistance in between of the interfaces.

Therefore, several studies [62, 63] demonstrated that self-healable polymers as SPEs applied in Li-metal batteries can guarantee a stable electrolyte-electrode contact and block the growth of Li-metal dendrites. Figure 2-1 represents the beneficial effect of the use of self-healable polymer electrolytes comparatively to a conventional SPEs. Hence, a poor SEI contact in batteries with general SPEs leads to an uneven Li-ion distribution on the Li-metal anode throughout the process of lithium plating and stripping. This can be easily overcome if having a stable interface built up by self-healable polymer electrolyte. Thus, the use of SPEs with self-healable properties result in an enhanced reliability of the battery assembly and extended lifetime of devices.

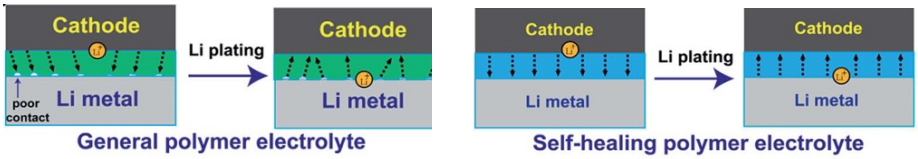

Figure 2-1 Schematic illustration of Li plating of conventional and self-healing polymer electrolytes on Li metal anode [63]

The recent discovery of a novel class of polymer materials known as vitrimers shed some light on the field of solid polymer electrolytes. Vitrimers possess unique features that

make them to be potentially considered ideal candidates for smart-batteries. They behave like thermoset polymer at ambient temperatures and flow like viscoelastic liquids at elevated temperatures. Moreover, vitrimers are self-healable and malleable. These properties underlie the interest to use vitrimers as a material for an electrolyte for solid polymer Li-ion batteries and Li-metal batteries as vitrimers comprise a number of beneficial properties that can help achieve high battery performance.

Vitrimer-like polymer-based electrolytes can provide good mechanical properties to support the battery assembly during working at RT and assure stable ion transport through SEI due to its self-healable nature. Additionally, vitrimer-like materials can be reshaped and thus, potentially reused which is especially crucial for further recycling and reuse pathways within a greener chemistry approach.

Overall, the strategy towards high performance all-solid-state batteries reasoned above would be used for the development of a novel solid polymer electrolyte with vitrimer-like behavior.

2.2 System inventory

The following master thesis work is to be devoted to the development of the solid polymer electrolyte design in which the cohesive and deformable properties of dynamic covalent polymeric network will be used. As it was earlier mentioned in Chapter I there are different vitrimer systems that exist. But hereby, inspired by several articles [59, 60] a room temperature self-healable cross-linked polymer system based on disulfide metathesis reaction was decided to be addressed.

2.2.1 Base polymer

Within the domain of synthesis of tailor-made polymer systems for SPEs, the scalability and the repeatability of the results are great issues. That is why within the scope of this master thesis only commercially available polymers were used.

As a base polymer for further research polymer grades produced by Nouryon such as Thioplast G44 and Thioplast G131 were used [64]. The chemical structure of a branched polymer and table with properties are presented below in Scheme 2.2-1:

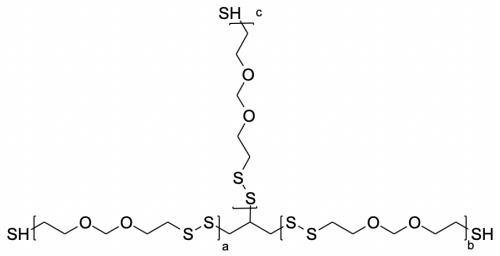

Scheme 2.2-1 Chemical structure of Thioplast G44 ($a + b + c < 5$) and G131 ($a + b + c = 31{\sim}38$).

Table 2-1 Technical characteristics of Thioplast grades [64]

	Units	**G44**	**G131**
Average MW	g/mol	$\leq$ 1100	$5200 - 6500$
SH-content relatively to MW	$wt\%$	$6.0 - 7.0$	$1.0 - 1.3$

Thioplast polymeric system was chosen as it satisfied a list of requirements for the particular design of SPE which was earlier proposed:

1) oligoethylene oxide polymer backbone participates in the dissolution of lithium salt and propels the Li-ion conduction throughout the medium;

2) disulfide bond induces vitrimer-like properties via disulfide metathesis reactions [57];
3) thiol-end groups can be used for the network formation via nucleophilic addition reaction.

2.2.2 Chemical cross-linking

Numerous benefits of the cross-linked polymer electrolytes were highlighted in the previous sections of the following manuscript. Not only does the cross-linked network enhance lithium-ion conductivity and improve the mechanical properties of SPEs, but it hinders the lithium dendrite growth as well.

In order to get a network, Thioplast polymer is to be chemically cross-linked via thiol-epoxy nucleophilic addition reaction with poly(ethylene glycol) diglycidyl ether (PEGDE) with average MW of $500\,g/mol$ promoted by $1\,wt.\%$ of 4-dimethylaminopyridine (DMAP) [59, 60]. The scheme of this chemical reaction is demonstrated below in Scheme 2.2-2:

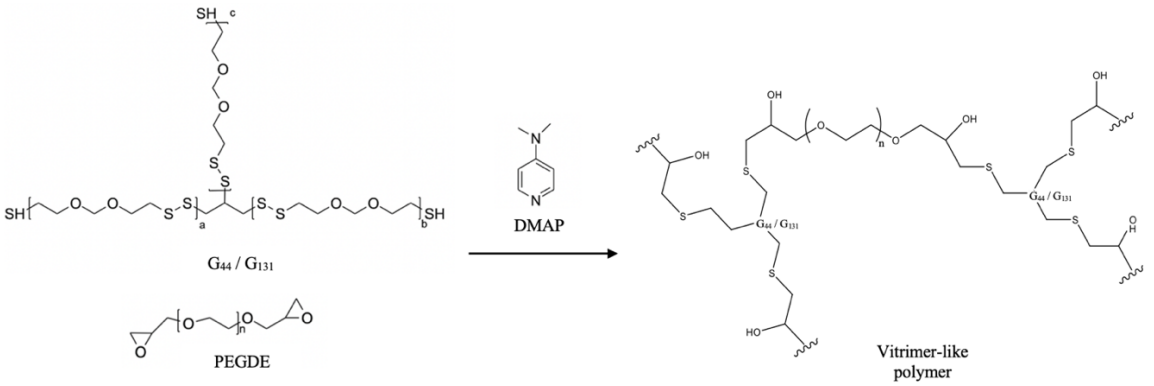

Scheme 2.2-2 Chemical cross-linking of Thioplast.

2.2.3 Disulfide metathesis

Vitrimer-like disulfide polymer materials intrinsically possess a self-healing functionality due to the presence of reversible chemical bonds [57]. Nevertheless, additional chemicals might be added to enhance the rate of the dynamic exchange of covalent associative bonds known as disulfide metathesis reactions. Metathesis can be understood as a dynamic transposition of the bonds [65].

Thus, it was successfully demonstrated that addition of the tributylphosphine (TBP) into the polymer bulk would extrinsically improve the self-healing properties as TBP agent will favor disulfide metathesis [60, 66]. The disulfide metathesis mechanism is presented in Scheme 2.2-3:

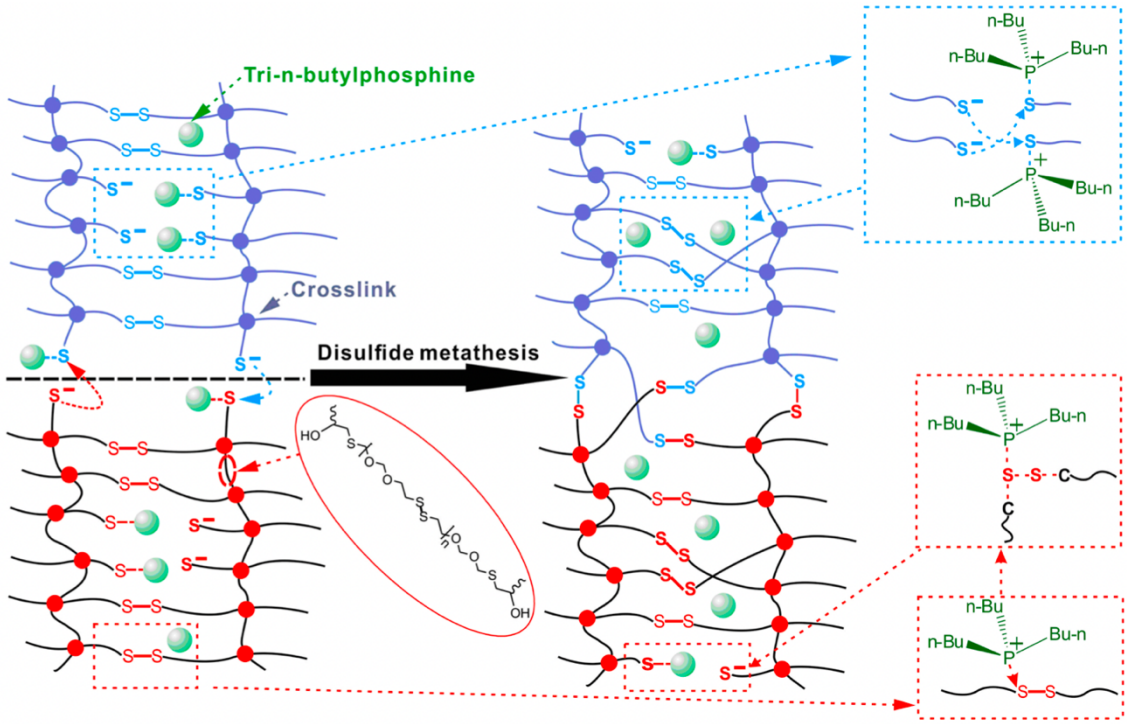

Scheme 2.2-3 TBP-catalyzed disulfide metathesis reaction within a polysulfide-based polymer network [60].

In accordance with the proposed mechanism, the addition of TBP leads to the formation of transient states between organophosphorus compound and disulfide bonds present in Thioplast polymer. These intermediates configurations comprise thiolate anions and phosphine salt cations which are generated on the macromolecular chain units. Therefore, this chain segmental movement at RT results in cross-nucleophilic attack. This occurs when thiolate anions switch to other sulfur atoms through TBP salt cationic intermediates. Hence, leading to a constant dynamic exchangeable network. Constant shuffling and rearrangement of the network at the macromolecular level engenders structural malleability at macro level. This allows to reshape the system.

2.3 Research methodology

A system inventory was introduced in the previous sections. As well, a detailed reasoning behind its selection was brought up to the attention of the reader to highlight the interest of the development of the vitrimer-based polymer system for the use as solid polymer electrolyte in LIBs.

The methodology of the research is going to be divided into several stages:

i. Analysis of the base products and evaluation of the electrochemical performance of polymer electrolytes based on non-cross-linked Thioplast grades;

ii. Development of the cross-linking protocol for Thioplast polymer grades;

iii. Verification of the self-healable properties of cross-linked polymeric network.

iv. Development of the processing route for electrolytes fabrication with further evaluation of their electrochemical performance.

The following analysis techniques are to be used within the scope of this research and the presented above methodology:

Spectroscopy

- FTIR
- Raman

Thermal Analysis

- DSC
- TGA

Electrochemical Analysis

- EIS

Optical analysis

- OM

In the end, based on the obtained data a conclusion about the potential of the polymer system based on Thioplast should be made. This is to evaluate whether the particular system described in the inventory should be further studied and used in SSB prototypes.

Chapter 3

Experimental section

3.1 Materials

All reagents were used as received.

Thioplast G44 and G131 were provided by Nouryon [64]. The most significant properties within the framework of this research were stated in Table 2-1.

PEGDE (average MW=500 g/mol, $d = 1{,}125\ g/ml$), LiTSFI (MW=287,09g/mol, >99.0%), $LiClO_4$ (MW=106,39 g/mol, >95.0%) were supplied by Sigma Aldrich.

DMAP was bought from TCI (MW= $122{,}17 g/mol$, >99.0%).

THF was purchased from VWR Chemicals BDH (MW=$122{,}17 g/mol$, T_b=66 ℃, $d = 0{,}89\ g/ml$, >99%).

3.2 Preparation of the cross-linked G44 and G131 networks

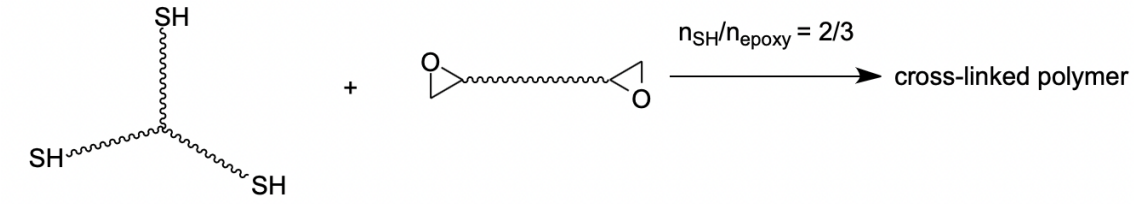

Scheme 3.2-1 Simplified scheme of the cross-linking reaction.

The amount of crosslinker, PEGDE, was added either to G44 or G131 to give a ratio of $n_{SH}/n_{epoxy} = 2/3$. After which, the cross-linking reaction promoter, DMAP, and disulfide exchange reaction catalyst, TBP, were added to the system by 1 % and 0,3 % relative to the total mass.

Preparation of the cross-linked network

Thioplast (1 mmol) was introduced into a 10 mL vial. On the side, PEGDE (1,5 mmol for G44 and 0,66 mmol for G131) was weighted in a 5 mL vial into which DMAP, 1 % relative of the total mass, was added. The mixture was then dissolved in the minimum amount of THF (0,1 mL). Some of the samples were prepared with 0,3 wt. % of TBP. The homogeneous obtained mixture in the 5 ml vial was then transferred to the 10 mL vial containing Thioplast and been stirred manually with a spatula. Further, samples were thermally cured in the vacuum oven for 2 days at 40 ℃ followed by 2h at 60 ℃. The curing conditions were adjusted from an article focusing on a similar system [60].

3.3 Preparation of G44 and G131 electrolytes

Prior to deepening into the procedure of electrolyte preparation, it should be mentioned that electrolyte samples were initially planned to be prepared with $LiTFSI$ and some batches of electrolyte were prepared with it in a glovebox environment. But targeting sample preparation in more accessible conditions, which will decrease the operation difficulty and the cost, another salt, $LiClO_4$, was used. Furthermore, some electrolyte samples were tested in swageloks and some in coin cells. This was due to the limited

availabilities of swageloks' assemblies and considerations about better temperature conduction (as for coin cells).

3.3.1 Non-cross-linked polymer electrolyte

The electrolyte preparation based on the bare Thioplast polymers was performed in accordance with the following procedure.

Preparation of the non-cross-linked polymer electrolyte

Different quantities of lithium salts were dissolved in THF and further introduced to the dissolved in THF Thioplast polymers. The preparation of samples with $LiTFSI$ was performed in an argon glove box, while with $LiClO_4$ in air atmosphere. The amounts of lithium salts were determined either by weight percentage or according to the n_{ether}/n_{Li^+} ratio respectively.

The mixture was stirred overnight to insure a complete homogenization. Moreover, the electrolytes with different lithium salt content were transferred to the swagelok contact surfaces or spacers covered with PTFE (Teflon) glass-reinforced separator (thickness – $126\ \mu m$, contact area – $0{,}506\ cm^2$). The separators were used to prevent cell shorting through direct contact of the poles because prepared electrolytes (shown in Figure 3-1) could not assure sufficient mechanical properties to withstand the pressure applied during the swagelok / coin cell assembly.

Figure 3-1 Different ratios of G44 / LiTSFI based non-cross-linked electrolytes.

Electrolytes were prepared via drop-casting. Therefore, a solution of polymer salt in Thioplast was dropped onto the stainless-steel surfaces of either swageloks or spacers. Afterwards, samples were transported to the vacuum oven for a complete evaporation of THF ($70°C$ for 24h). The dried samples were then transferred back to the glovebox for the assembly of the electrochemical cells. The assembled cells were subjected to the electrochemical impedance spectroscopy testing (EIS) at RT and at variable temperatures for evaluation of the system performance.

3.3.2 Cross-linked polymer electrolyte

Solid-state-polymer electrolytes were prepared via two major processing routes. The first major procedure was based on the synthesis of electrolytes via direct in-mold cross-linking reaction. Several challenges were faced with this procedure. Therefore, a second methodology was developed by adjustment of solvent content, mixing, casting and curing procedures. Figure 3-2 shows clearly the difference between the two types of electrolytes prepared via two different ways.

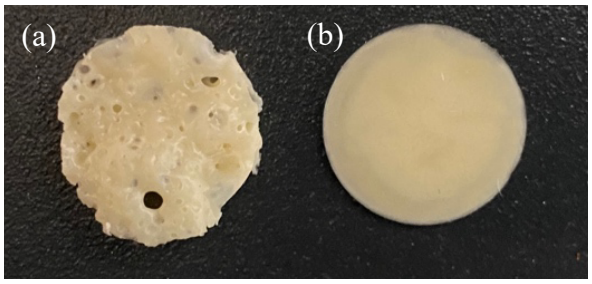

Figure 3-2 Cross-linked solid polymer electrolytes G131-based prepared via (a) direct in-mold cross-linking and (b) drop-casting methods.

Protocol (A): preparation of the cross-linked electrolyte via direct in-mold cross-linking

Thioplast was weighted in a 25 mL Teflon mold. Aside, DMAP, PEGDE and TBP were dissolved in THF as described in section 3.2. Separately, lithium salt was dissolved in THF and stirred until obtaining a homogeneous solution. The final step of the procedure comprised of the mixing of the two pre-prepared solutions with Thioplast in the Teflon mold with subsequent stirring with a spatula. Afterwards, samples were thermally cured in a vacuum oven for 2 days at 40℃ and 2h at 60℃. Thus, a film with a thickness of 1,5 mm and 3 cm as a diameter was obtained. Electrolytes for testing were cut as of the metal spacer size with a diameter of 1,58 cm.

Protocol (B): preparation of the cross-linked electrolyte via drop-casting

The difference between Protocol (A) and (B) is that in the latter one, Thioplast was dissolved in THF before mixing it with the other reactants and dissolved lithium-salt. The obtained slurry was then dropped onto the contact surfaces and subjected to the thermal curing. Conditions of the curing were as follow: 2 days at RT, 1 day at 40℃ in an oven and 2h at 70℃ in a vacuum oven. In the end films with 1,58 cm diameter of 700 μm thickness were obtained.

The electrolytes prepared via two ways were finally transferred to the glovebox for the assembly of the electrochemical cells.

3.4 Swagelok / coin cell assembly

Swageloks and coin cells were assembled in an argon atmosphere in the glove box in accordance with the schemes presented below:

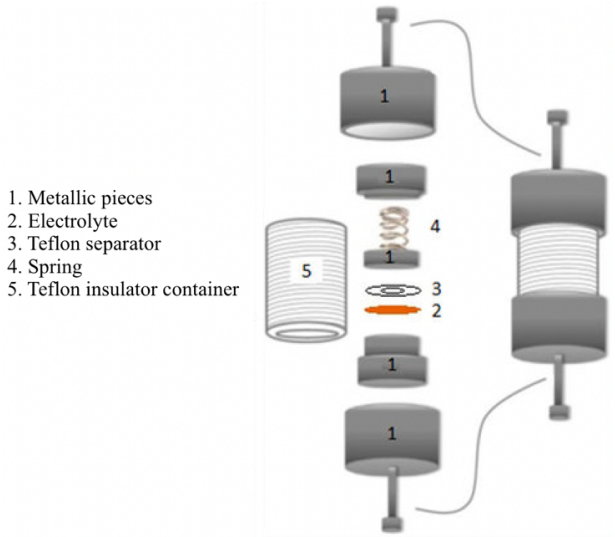

Scheme 3.4-1 Swagelok cell assembly for EIS measurements [67].

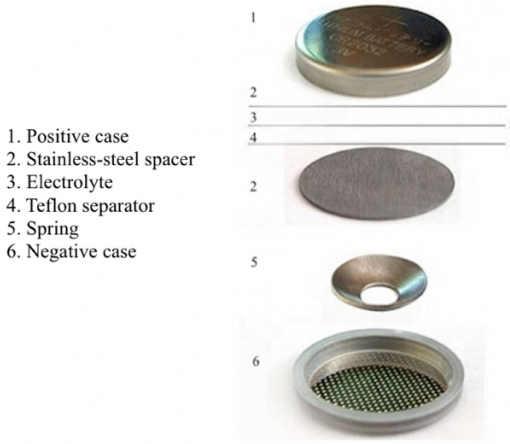

Scheme 3.4-2 Coin cell assembly for EIS measurements [68]

Teflon separators were not required for the cells assembly if electrolytes provided sufficient mechanical properties.

At the final stage, swagelok assemblies should be tightly screwed manually, while coin cells should be crimped in a hydraulic crimping machine.

Chapter 4

Equipment

The following chapter briefly describes analysis techniques and equipment used during the performed master thesis work.

4.1 Spectroscopy

Fourier transform infrared (FTIR) spectroscopy was used to attribute functions to the chemical structure of polymers. The spectra were recorded on Microscope FTIR Nicolet IN10 with MCT (MCT (Mercury-Cadmium-Telluride) detector. The samples were subjected to 64 acquisitions with 4 cm^{-1} resolution. Non-transparent samples were analyzed with micro-attenuated total reflection (ATR) technique on germanium tip with an applied force on the surface of 15 N.

Raman spectroscopy was performed to put in evidence the existence of the disulfide bond for non-cross-linked and cross-linked samples after curing. The technique was executed on Thermo-fisher Raman DXR coupled with Continuum microscope. The studied samples were subjected to 10 acquisitions with laser of 532 nm wavelength through a 50 μm pinhole aperture.

4.2 Thermal analysis

Differential scanning calorimetry (DSC) was used to determine glass transition temperature T_g of the polymer. DSC measurements were carried out using a Mettler Toledo 822e calorimeter. The samples were analyzed under nitrogen atmosphere with the flow of 50 mL/min in aluminum (Al) pan with an empty aluminum pan as reference cell. The samples were subjected to initial heating from -80 °C to 120 °C then cooled down to -80 °C, and reheated up to 120°C with a 10 °C/min heating/cooling rate. Two heating cycles were run to confirm the completeness of the curing reaction.

Thermo-gravimetrical analysis (TGA) was carried out to determine the thermal stability of polymers with their decomposition temperatures. The equipment used: TGA/SDTA 851e by Mettler Toledo. The tests were performed under nitrogen atmosphere in a 50 mL/min, in alumina crucibles with volume of 70 μl. The samples were subjected to heating from 30 °C to 600 °C with a 10 °C/min heating rate.

4.3 Optical analysis

Optical microscopy (OM) was performed in order to investigate self-healable properties of the dynamic network. The analysis was carried out on a AX70 microscope from Olympus coupled with an in-built HD camera.

4.4 Electrochemical analysis

Electrochemical impedance spectroscopy (EIS) allowed to obtain the data about the ionic conductivity of synthesized electrolytes (the details of calculations would be clarified later). EIS measurements were performed using a VMP-300 Potentiostat

apparatus from BioLogic over a frequency range of 7 MHz to 100 mHz and with an amplitude AC excitation voltage of 10 mV. The electrochemical cells were placed into the temperature chamber. Thus, the electrochemical impedance spectra were collected for a temperature range from 60 °C to 10 °C by gradually decreasing the temperature by steps of 10 °C with an equilibration time of 1h between each measurement.

Chapter 5

Experimental results and discussion

The following chapter comprises the comparison of the non-cross-linked and cross-linked system (prepared in accordance with protocols from Chapter III).

5.1 Characterization of structure

5.1.1 FTIR spectroscopy

Firstly, FTIR analysis was performed to confirm the structure of polymers before and after cross-linking. Spectra of G44-based system are presented in Figure 5-1. Spectra of G131-based system are presented in Figure 5-2.

In accordance with the absorption peaks appearing at the spectra in Figure 5-1 the following structural characteristics were identified both for non-cross-linked G44 and cross-linked samples: C-H stretching at the 3000-2840 cm^{-1}, C-H bending at 1470-1450 cm^{-1}, -C-H rocking at 1370-1350cm^{-1}, C-O stretching at 1150-1080 cm^{-1}. The peak that can be ascribed to C-S stretch (at 730cm^{-1}) is very weak. While S-S stretch (at 550cm^{-1}) cannot be seen in FTIR spectra registered on the equipment used (see technical characteristics in Chapter IV).

Nonetheless, the below spectra clearly prove that the chemical reaction between thiol-end groups and epoxy proceeded successfully. This conclusion was made based on the further considerations: S-H stretching absorption peak at 2575 cm^{-1} disappeared for the cross-linked sample, whilst O-H stretching peak at 3450 cm^{-1} appeared after the epoxy-ring-opening reaction. It can be noticed that a peak corresponding to C=C at 1650 cm^{-1} appeared for the cross-linked samples. The peak can be attributed to the double bond carried by DMAP.

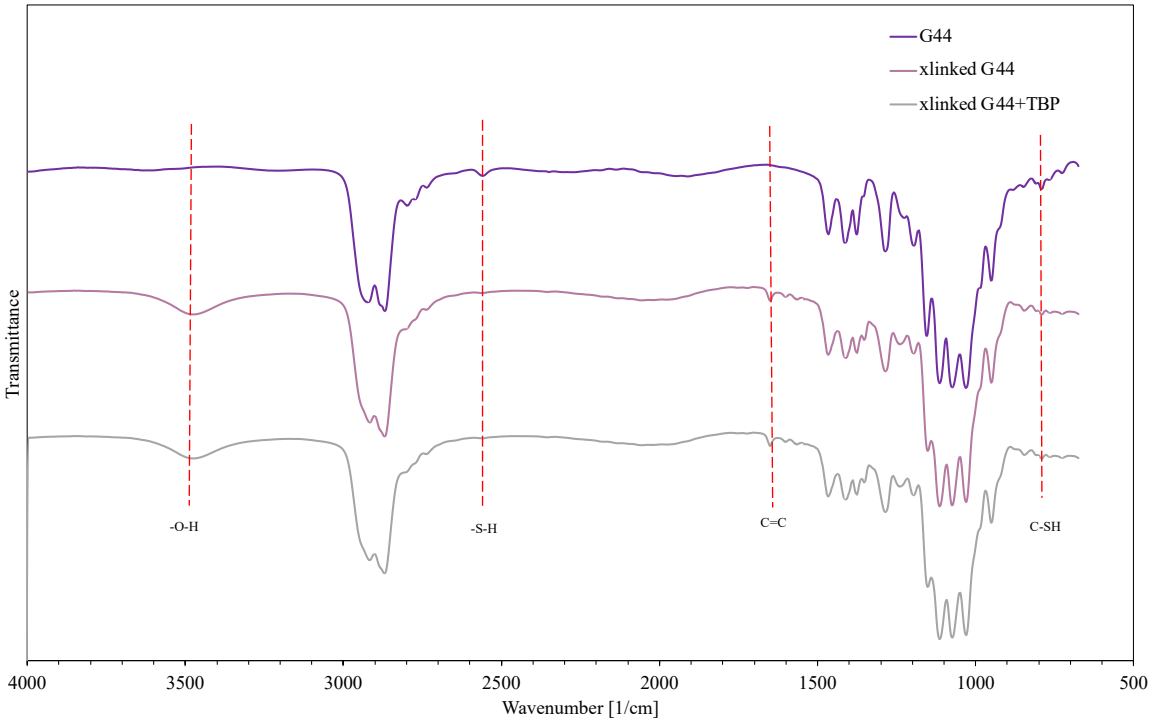

Figure 5-1 FTIR spectra of G44-based systems: non-cross-linked G44, cross-linked G44 (without and with TBP).

Spectra of G131-based system presented in Figure 5-2 were obtained by ATR FTIR mode as the cross-linked samples were not transparent and exhibited sufficient mechanical properties to withstand the pressure from the Germanium crystal tip.

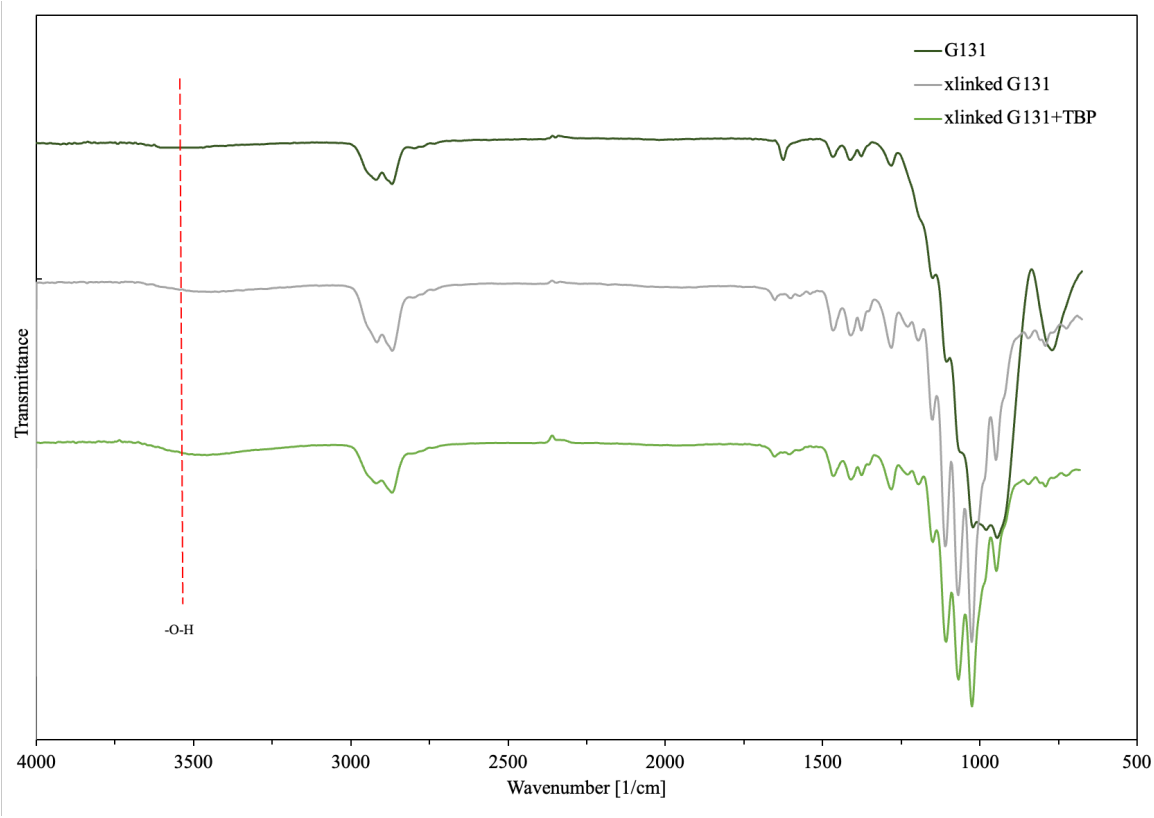

Figure 5-2 FTIR spectra of G131-based systems: non-cross-linked G131, cross-linked G131 (without and with TBP).

However, the obtained for the G131-based system spectra are less informative than the ones for the G44-based systems. This is because peaks from thiol end-groups cannot be observed and the conclusion about the consumption of the S-H throughout reaction cannot be made. Additionally, we are not sure whether the stretch peak referring to O-H group at 3450 cm^{-1}, which should appear after the epoxy-ring-opening reaction, was presented in the curves. This might be due to the fact that Thioplast G44 is a grade which contains the highest amount of -SH end groups by weight among Nouryon's Thioplast grades (as mentioned in Table 2-1); and in particularly G131. Hence, the signal from thiol groups for the G44-based systems can be very strong and thus clearly seen. While for the

G131-based systems the S-H signal might be below the detection limit of the used set-up. As well, the reason why the signal from S-H is not obvious for the G131 samples might be due to the different modes used for the measurements.

Since FTIR did not help to unequivocally justify the crosslinking for the G131 system, Raman was performed as a complementary analysis.

5.1.2 Raman spectroscopy

Disulfide bonds are essential for introducing vitrimer-like behavior to the network. This is to say that the S-S bonds in the non-cross-linked polymers should withstand cross-linking reaction and thermal curing conditions to be still present in the synthesized network. As the recorded FTIR spectra could not justify the stability of the disulfide bond, Raman spectroscopy was performed to put in evidence the S-S and C-S bonds.

Spectra of G44-based systems are presented in Figure 5-3. Spectra of G131-based systems are presented in Figure 5-4. The obtained spectra were analyzed by monitoring of the changes at the following Raman shifts, which were of the main interest within the scope of my research: S-H stretch vibrations 2550 - 2600 cm^{-1}, C-S stretch vibrations 630 – 790 cm^{-1}, S-S stretch vibrations 430 -550 cm^{-1}.

Based on the presence of C-S and S-S peaks in the system before and after cross-linking of the polymer, it can be concluded that the disulfide bond was conserved throughout the chemical reaction and thermal curing. It means that we can expect to observe the vitrimer-like behavior in the studied systems.

Additionally, Raman analysis, complementary to FTIR, put in evidence that chemical reaction took place: corresponding to thiol-end groups peaks disappeared in the spectra for the samples after cross-linking.

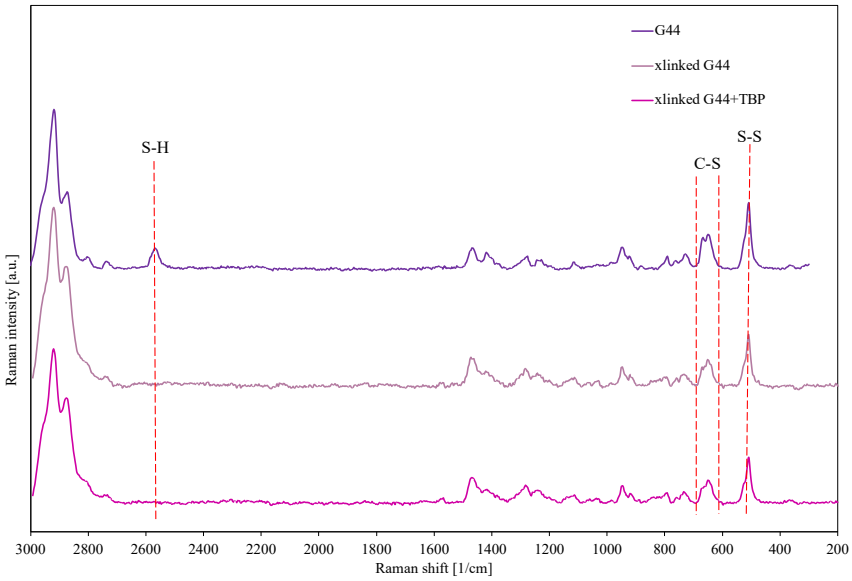

Figure 5-3 Raman spectra of G44-based systems: non-cross-linked G44, cross-linked G44 (without and with TBP).

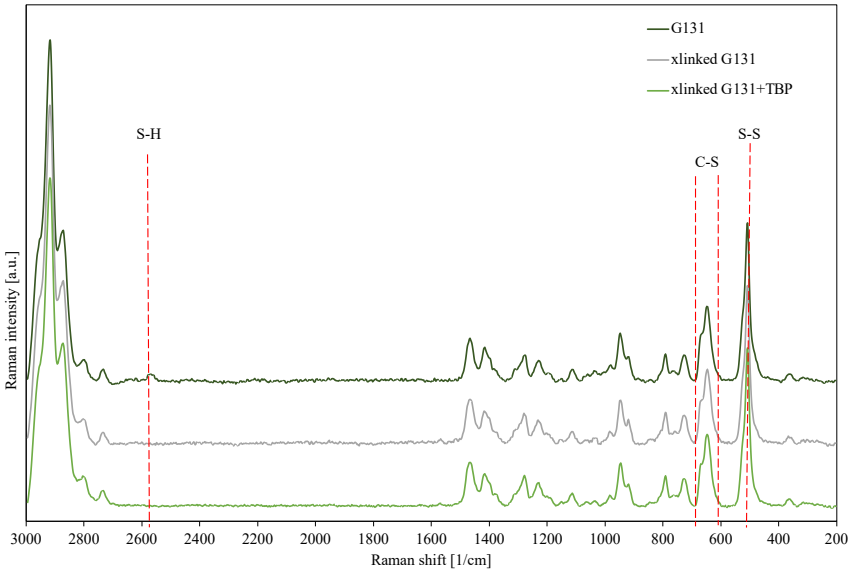

Figure 5-4 Raman spectra of G131-based systems: non-cross-linked G131, cross-linked G131 (without and with TBP).

5.2 Thermal properties

Thermal properties of the Thioplast systems were investigated in order to determine essential characteristics of the polymer, such as glass transition temperature T_g and temperature of degradation.

5.2.1 DSC

DSC heating curves for G44 and G131 - based systems are presented in Figure 5-5 and Figure 5-6 respectively. Both systems undergo only one transition from glassy to rubbery state at T_g, no melting and crystallization transitions were observed. This indicates the amorphous nature of polymers.

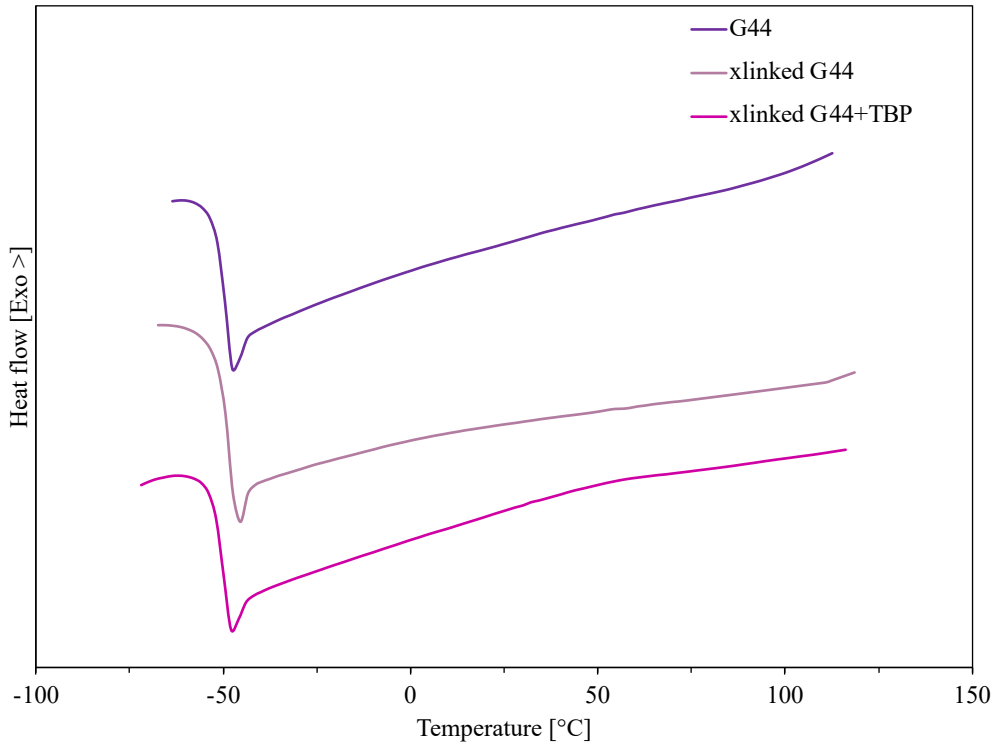

Figure 5-5 DSC heating curves for G44-based systems: non-cross-linked G44, cross-linked G44 (without and with TBP).

T_g was calculated with corresponding software by using a half-height technique in the transition region. Thus, the T_g of the non-cross-linked G44 polymer is -49 ℃, while for the cross-linked is $T_g = -47$ ℃. The T_g of the non-cross-linked G131 polymer is -55 ℃, while for the cross-linked is $T_g = -51$ ℃.

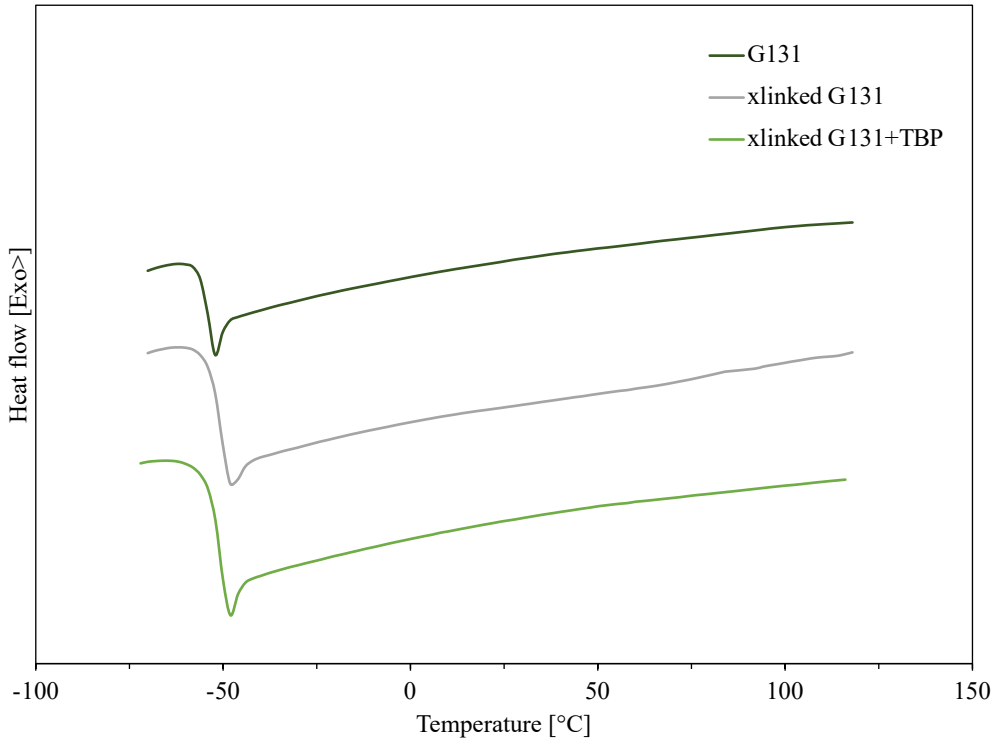

Figure 5-6 DSC heating curves for G44-based systems: non-cross-linked G44, cross-linked G44 (without and with TBP).

The glass transition temperatures of the non-cross-linked polymers correspond to the information from the manufacturer [64]. Additionally, it is worth to mention that it was observed that T_g slightly increased with increase of the polymer molecular mass and crosslinking. This happened due to the decrease of the chain segmental mobility that can be attributed both to the increase of the molecular mass and to the creation of the network.

5.2.2 TGA

The thermal degradation and stability investigation of Thioplast polymeric systems (as received) was performed with TGA. The obtained results are shown in Figure 5-7.

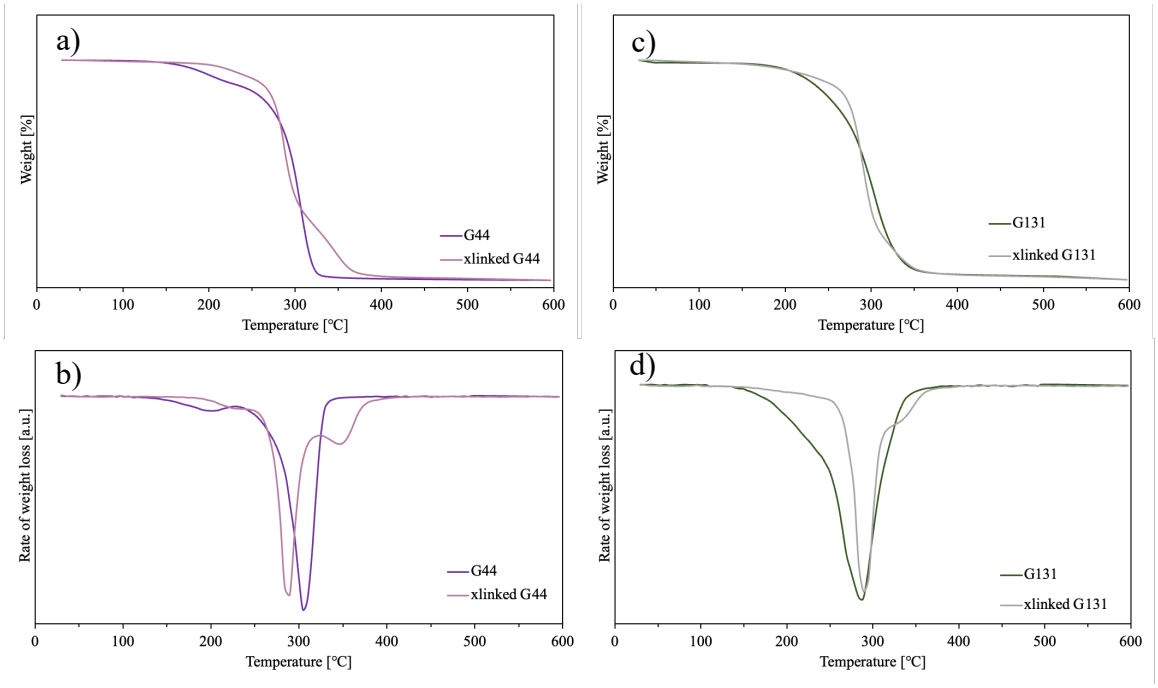

Figure 5-7 (a) TGA and (b) DTG curves for G44-based systems; (c) TGA and (d) DTG curves for G131-based systems.

Based on the obtained results, we can deduce that Thioplast polymers and products based on it are thermally stable up to 200 °C. It is important to mention that no weight loss at 66 °C, that can be attributed to the evaporation of THF, was observed. Meaning that all THF was evaporated during the curing step.

For non-cross-linked G44 there are two mass decreasing peaks: 130 °C and 218 °C. The first mass decrease could be attributed to the decomposition of the shorter or broken chains. The second one could be related to the decomposition of the main three-arm chains.

The cross-linked polymer starts decomposing later at 210 °C and show three decomposition processes.

Concerning non-cross-linked G131, one gradual decomposition from 150 °C can be observed. This is due to the possibility of presence of chains with different lengths. The cross-linked samples presented better stability, degradation at 220 °C and having three decomposition processes.

Overall, for both systems, cross-linking process leads to a delay in the degradation process due to the development of a more stable network rather than for non-cross-linked polymers.

5.3 Self-healing performance

The cross-linked system was expected to exhibit self-healable properties at RT. To prove it, we performed optical microscopy for the most promising samples: cross-linked G131 with and without TBP. These cube-shaped (5 mm^3) samples were cut with a razor in a V-shaped way. Then the self-healable behavior was monitored by means of taking photos with an in-built HD camera during time.

As shown in Figure 5-8 and Figure 5-9 the sample containing TBP was completely self-healed in 4 hours compared to the sample exempted from TBP which didn't self-healed even in 72 h. This puts in evidence the catalyzing effect of TBP on the dynamicity of the disulfide-exchange reactions.

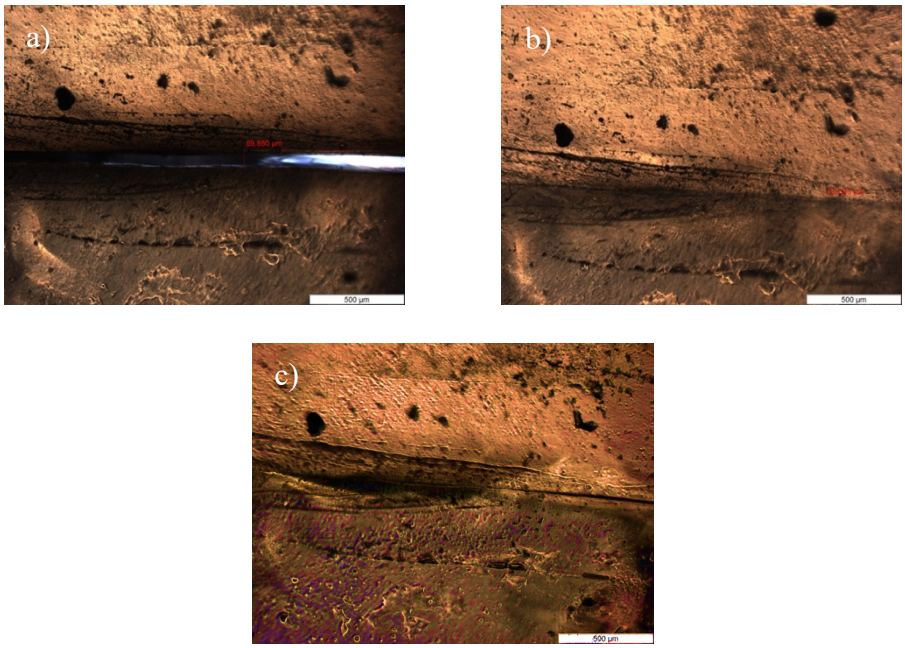

Figure 5-8 Optical images showing healing processes of a cross razor wound of G131 cross-linked with TBP after (a) 0 h; (b) 4 h; (c) 72 h.

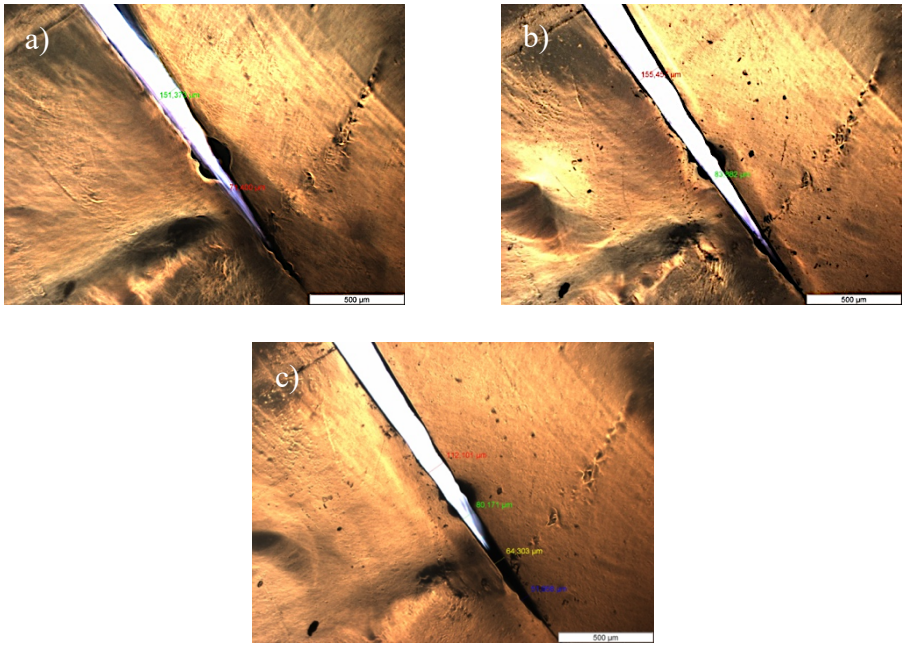

Figure 5-9 Optical images showing healing processes of a cross razor wound of G131 cross-linked without TBP after (a) 0 h; (b) 4 h; (c) 72 h.

5.4 Electrochemical analysis

The previous sections of Chapter V (sections 5.1. – 5.3.) primarily proved the formation of the network and extensively covered different properties attributed to it. In the following section of Chapter V, we are going to focus on the evaluation of the electrochemical performance of the electrolytes, meaning that polymer networks with no added salt would be no longer addressed.

The cells with electrolytes prepared in accordance with protocols in Chapter III (sections 3.3.1, 3.3.2) and assembled as described in section 3.4, were subjected to the electrochemical impedance spectroscopy testing. The resistance R_b extracted from the Nyquist diagrams was used later on to calculate the conductivity (σ) as shown in Equation (5-1), in which *A* stands for the area of the electrolyte sample in contact with the electrodes and t for the electrolyte thickness:

$$\sigma = \frac{t}{R_b * A} \tag{5-1}$$

5.4.1 G44-based electrolytes

Initially, the research started with the investigation of Thioplast G44 system. It seemed to be a very promising polymer to be used within the concept introduced in Chapter II. The conductivities of non-cross-linked electrolytes ($A = 0{,}5\ cm^2$ and $t = 0{,}0126\ cm$) with different mass ratios of LiTSFI to G44 were measured at RT in swageloks. The results are presented in Figure 5-10. As seen, the electrolyte with the lowest content of lithium salt (LiTSFI/G44 – 1:9) had the conductivity of $1{,}3 \cdot 10^{-5}\ Scm^{-1}$, which gradually increased with the increase of lithium salt content reaching $4{,}4 \cdot 10^{-5}\ Scm^{-1}$ (LiTSFI/G44 – 1:1).

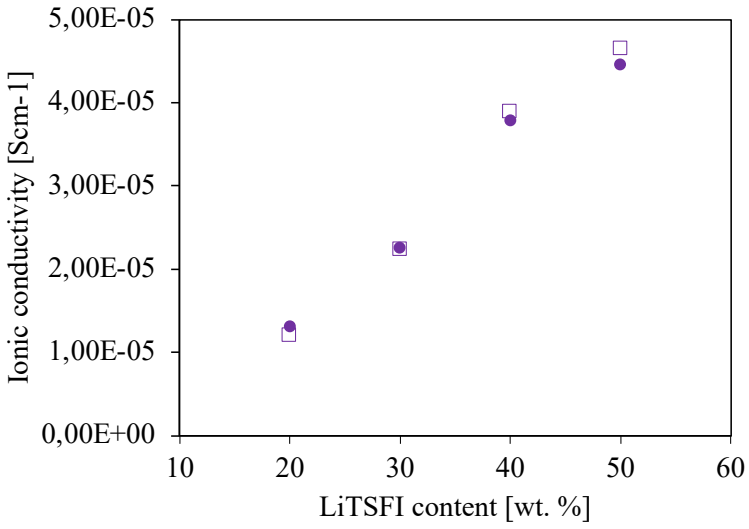

Figure 5-10 Room temperature conductivity of the G44–LiTSFI electrolytes as a function of LiTSFI concentration.

After this we started to make trials to cross-link Thioplast. The cross-linked polymeric network based on G44 didn't provide the expected mechanical properties for solid-state electrolytes. Even by increasing the content of crosslinker ($\frac{n_{epoxy}}{n_{SH}} > 3/2$), the system looked non-reliable to be implemented in a solid-state battery. This can be seen in the pictures of the cross-linked G44 comparatively to the non-cross-linked one (Figure 5-11) and cross-linked G131 (Figure 5-12).

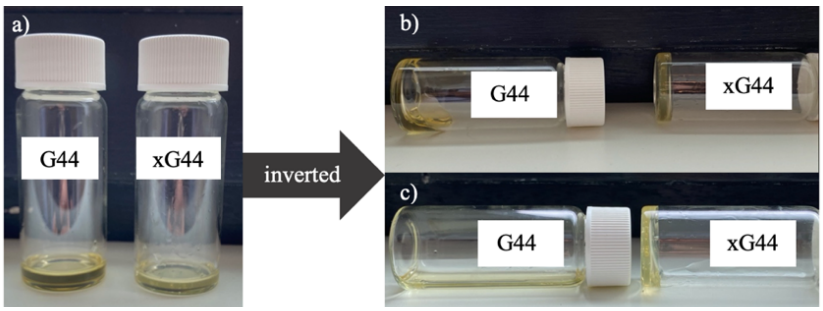

Figure 5-11 The behavior of G44 before and after cross-linking (xG44) when inverted after (a) t = 0 s; (b) t = 2 s and (c) t = 2 min.

Figure 5-12 Cross-linked G131.

This is the reason why the analysis of the G44-based systems was suspended. And further in-depth analysis proceeded with G131-based electrolytes.

5.4.2 G131-based electrolytes

The amount of lithium salt ($LiClO_4$) was taken according to the number of moles of ether groups (required for the conduction as explained in section 1.4.2.2.) to the number of moles of lithium-ion: n_{ether}/n_{Li^+}. The EIS was performed at different temperatures for electrolytes assembled in coin cells. The measured conductivities were plotted in $\log(\sigma)$ vs $1000/T$ coordinates.

Similarly to G44, the investigation of the G131-based system started with the EIS testing of the non-cross-linked electrolyte (see preparation procedure in section 3.3.1.). The results are presented in Figure 5-13. From the plot it can be observed that the conductivity increases with temperature. It can be attributed to the increase of the ion mobility. For the sample with n_{ether}/n_{Li^+} – 10/1 (27,6 wt. % of $LiClO_4$) the conductivity increased from $2{,}9 \cdot 10^{-6}\ Scm^{-1}$ at 20 °C to $1{,}2 \cdot 10^{-4}\ Scm^{-1}$ at 60 °C.

Moreover, a trend of the conductivity increase with the increase of the lithium salt content can be noticed. Therefore, the conductivity at 30 °C for the samples with

n_{ether}/n_{Li^+} – 15/1 (20,3 wt. % of $LiClO_4$) increased from $6{,}0 \cdot 10^{-6}\ Scm^{-1}$ to $8{,}5 \cdot 10^{-5}\ Scm^{-1}$ for the most performing one, here n_{ether}/n_{Li^+} – 10/1. The most loaded samples, n_{ether}/n_{Li^+} – 8/1 (32,3 wt. % of $LiClO_4$), showed lower conductivities than the samples with lower lithium salt contents. It might be attributed to the agglomeration of lithium salt which negatively affected conductivity in the prepared SPE.

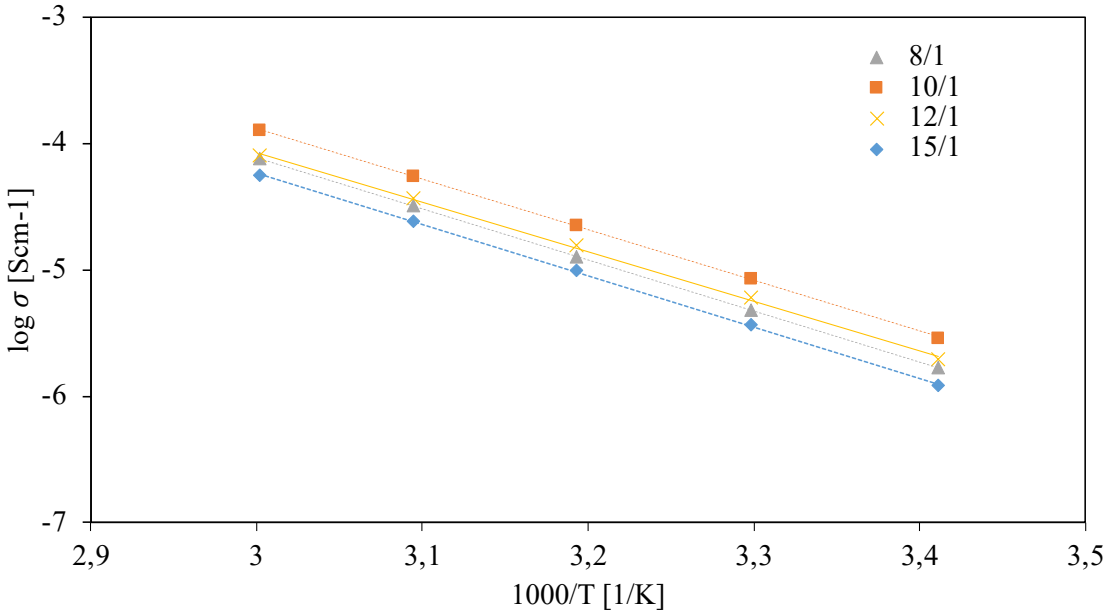

Figure 5-13 Temperature-dependent conductivity of non-cross-linked G131-based electrolytes for different n_{ether}/n_{Li^+} ratios.

Cross-linked G131-based electrolytes answered our expectations and satisfied the requirements on mechanical properties. That is why a number of complementary electrochemical tests was performed. As it was said in section 3.3.2., two different protocols of cross-linked electrolytes preparation were used: Protocol (A) and Protocol (B). Additionally, within each protocol, systems with and without TBP were investigated.

All obtained graphs are shown in Appendix A. Figure A - 1 and Figure A - 2 correspond to the electrolytes prepared according to Protocol (A). Figure A - 3 and Figure A - 4 show results of the conductivity for the electrolytes synthesized via Protocol (B).

Altogether, analyzing the compiled data, the general trends which were pointed out earlier, were confirmed. Therefore, conductivity gradually increases with temperature for all the analyzed batches of samples. In most cases, the conductivity increases with the increase of lithium salt content. The stable results were obtained for the following n_{ether}/n_{Li^+} ratios: 15/1, 12/1 and 10/1. However, very often samples with higher amounts of lithium salts, here $n_{ether}/n_{Li^+} - 8/1$, suffered from bad reproducibility of the results which could be accounted for the lithium agglomeration within the electrolytes. This could result in intrinsic instabilities in the ion-conduction process decreasing the conductivity.

Additionally, it should be mentioned that the higher conductivities were achieved with the films synthesized according to Protocol (B). The comparative graph for electrolyte films with $n_{ether}/n_{Li^+} - 10/1$ is presented in Figure 5-14. Films prepared as explained in Protocol (B) showed better thickness uniformity and didn't have visible macro-porosity (can be clearly seen in Figure 3-2). As well, none of the assembled cells with the latter electrolytes shorted throughout the analysis.

For the samples prepared via Protocol (B) the difference between samples with TBP and without couldn't be clearly stated based on the EIS results only. Therefore, if needed, additional investigation upon the influence of TBP addition into the system on electrochemical properties should be performed. The effect of TBP was more pronounced for electrolytes obtained as described in Protocol (A). It might be attributed to fact that

TBP catalyzed the self-healing behavior of the vitrimer-like polymer network (as confirmed in section 5.3.). By these means, the porosity could be healed and the homogeneity of the films could be improved. If so, the effect would be less noticeable if the electrolyte films were already homogeneous. This assumption was confirmed for the electrolytes obtained with the procedure stated in Protocol (B).

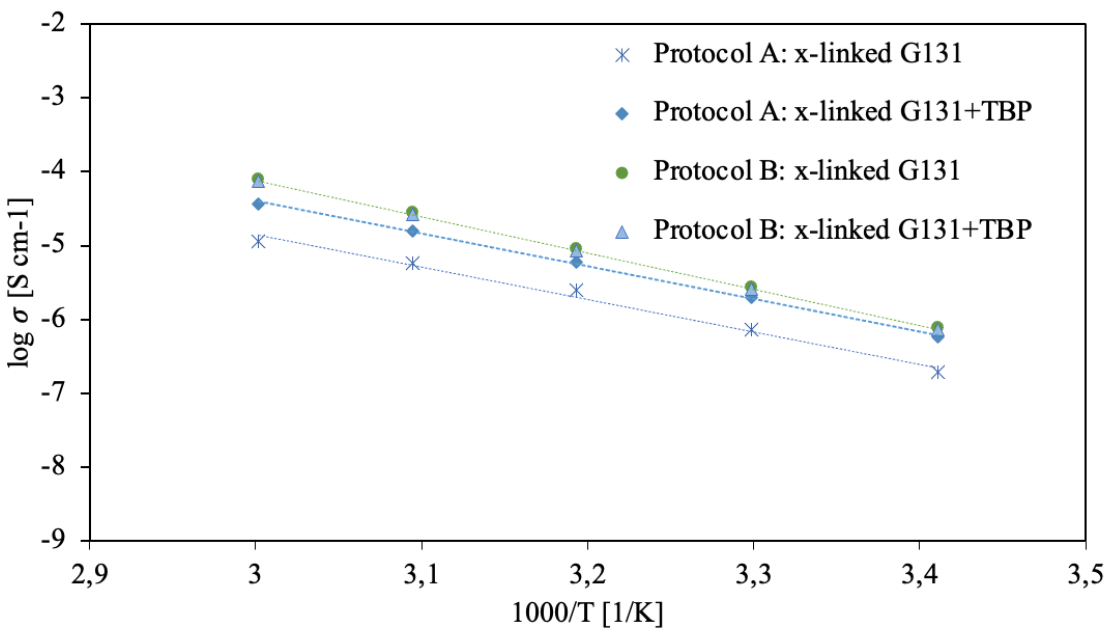

Figure 5-14 Temperature-dependent conductivity of cross-linked G131-based electrolytes prepared either according to Protocol (A) or Protocol (B) with a $n_{ether}/n_{Li^+} - 10/1$ ratio.

Hereby, to the attention of the reader, we decided to bring up and discuss only the most promising cross-linked samples comparing them with the non-cross-linked G131 electrolytes. Thus, the electrolytes with n_{ether}/n_{Li^+} – 10/1 (26,3 wt. % of $LiClO_4$) prepared via Protocol (B) were chosen for this reason and compared with non-cross-linked electrolytes with the same n_{ether}/n_{Li^+} ratio (for non-cross-linked electrolytes n_{ether}/n_{Li^+}

– 10/1 corresponds to 27,6 wt. % of $LiClO_4$). The ratio of n_{ether}/n_{Li^+} – 10/1 was chosen because it represented a good trade-off between the acceptable conductivity at moderate lithium salt loading.

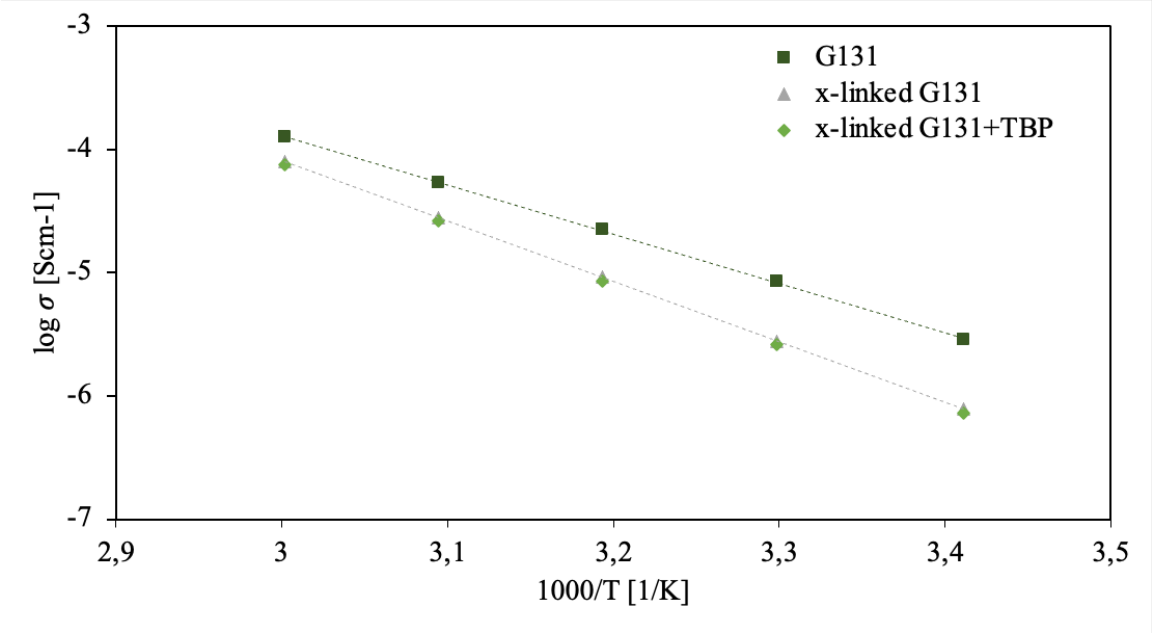

Figure 5-15 Temperature-dependent conductivity of G131-based electrolytes with n_{ether}/n_{Li^+} – 10/1. Electrolytes: non-cross-linked, cross-linked without TBP and cross-linked with TBP

The above Figure 5-15 shows that the non-cross-linked electrolytes present higher conductivities than the cross-linked ones. At higher temperature this difference is less pronounced as for the lower temperatures. The conductivity of the non-cross-linked electrolytes at 60 °C is only 1,7 times higher than the one of the cross-linked samples ($1{,}3 \cdot 10^{-4}\ Scm^{-1}$and $7{,}6 \cdot 10^{-5}\ Scm^{-1}$ correspondingly), while at 20 °C it is almost 4 times higher ($2{,}8 \cdot 10^{-6}\ Scm^{-1}$and $7{,}3 \cdot 10^{-7}\ Scm^{-1}$ correspondingly). This indeed can be expected.

First of all, non-cross-linked polymers hinder ion transport at lower extent than the cross-linked electrolytes. Nevertheless, the non-cross-linked electrolytes have a paste-like consistency, meaning that they cannot assure the expected mechanical properties and additional elements, as separators, should be used. While the cross-linked electrolytes provide moderate conductivities and sufficient mechanical properties to avoid electrode-electrode contact.

Moreover, the less noticeable difference of conductivities at higher temperatures can be attributed to the fact, that vitrimer-like polymers act like viscoelastic liquids when the associative exchange reactions are triggered by an increase in temperature. Therefore, the ion transport might be facilitated for the cross-linked electrolytes at elevated temperatures.

To conclude, the electrolytes prepared via a modified path (Protocol (B)) showed very good mechanical properties and acceptable ion-conducting properties and could be potentially used at elevated temperatures (higher than 50 °C) when conductivities are of the range of $10^{-5}\ Scm^{-1}$. To use these types of electrolytes at RT, the in-depth analysis should be continued. The effect of TBP content on the ionic conductivity and the electrochemical stability of electrolytes should be investigated.

Chapter 6

Conclusion and outlook

This master thesis aimed the synthesis of solid electrolytes based on vitrimer-like ionically-conducting polymers with subsequent characterization. Therefore, within the framework of this research, three main goals were targeted. The first part consisted of the development of the methodology for the polymer network formation via thiol-epoxy ring-opening reaction. The second part was devoted to the adaptation of the cross-linking procedure for the electrolytes processing. And finally, evaluation of the electrochemical performance of the prepared electrolytes with EIS.

Hence, the suitable conditions for polymer network synthesis were found and the reliable polymer networks were obtained. The stability of the disulfide bond, essential for inducing vitrimer-like behavior to the system, was confirmed. It is present in the medium after the cross-linking and thermal curing steps. Based on the developed cross-linking procedure, the conditions were adapted for solid-state polymer electrolytes preparation. The synthesized films showed reproducible results in terms of conductivity.

Additionally, a very particular feature, self-healing behavior due to the dynamic exchange reactions between disulfide bonds, was put in evidence. This property can be very beneficial when used in SPEs. Furthermore, ‘smart’ self-healable electrolytes can help hinder the growth of lithium dendrites. Therefore, high-capacity lithium metal anodes can be safely used in full cells.

Overall, the objectives of this master's thesis have been successfully fulfilled. Nevertheless, some improvements can be still made if proceeding further with investigation of the Thioplast systems. As it was mentioned, polymer network based on cross-linked Thioplast G44 did not provide the expected mechanical properties. However, in accordance with the information from Nouryon, Thioplast manufacturer, G44 is supposed to be used as a crosslinking agent itself. Therefore, G44 can be used with other Nouryon products which are disulfide functionalized epoxy resins e.g., EPS25 [64]. By these means, other systems containing disulfide bonds both in the main polymer and the cross-linker could potentially provide outstanding results in terms of conductivity and self-healable properties.

Moreover, the scope of the research can be extended towards the modification of the cathode materials in order to increase affinity between cathode and solid electrolyte and benefit from the improved ionic conductivity. The development of the cathode composition based on the same polymer as electrolyte with self-healable properties, can help overcome the problem of desintegrity. That is why vitrimer-like polymers, inherently exhibiting self-healable properties, can be considered as a very promising polymer system. And at the end, the full cells with lithium metal anode, modified cathode and vitrimer-like polymer electrolyte can be used for SSB prototyping.

APPENDIX A

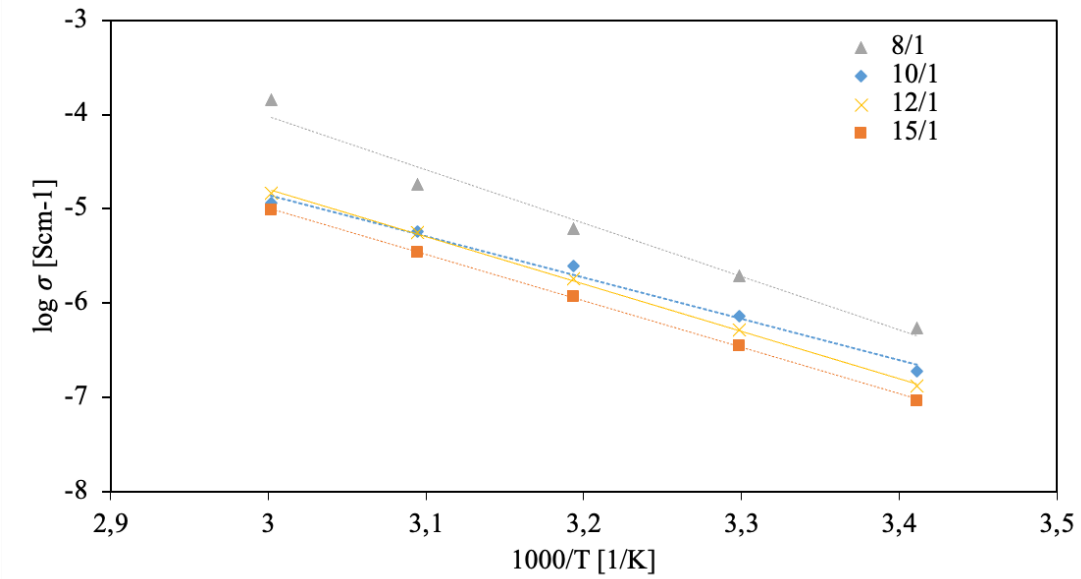

Figure A - 1 Temperature-dependent conductivity of cross-linked G131-based electrolytes without TBP (prepared via Protocol (A)) for different n_{ether}/n_{Li^+} ratios.

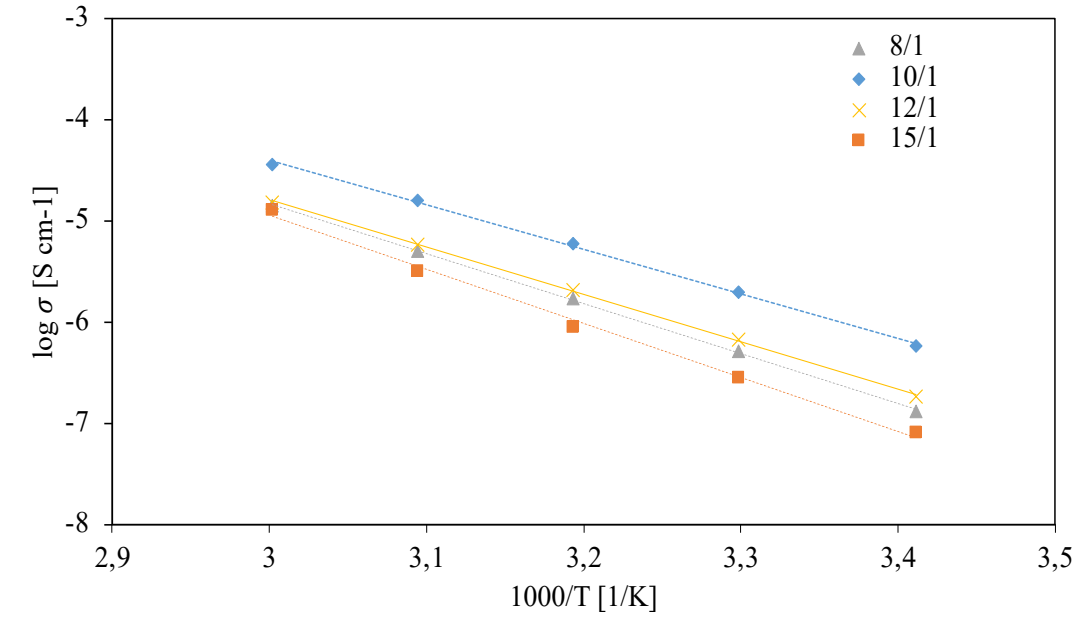

Figure A - 2 Temperature-dependent conductivity of cross-linked G131-based electrolytes with TBP (prepared via Protocol (A)) for different n_{ether}/n_{Li^+} ratios.

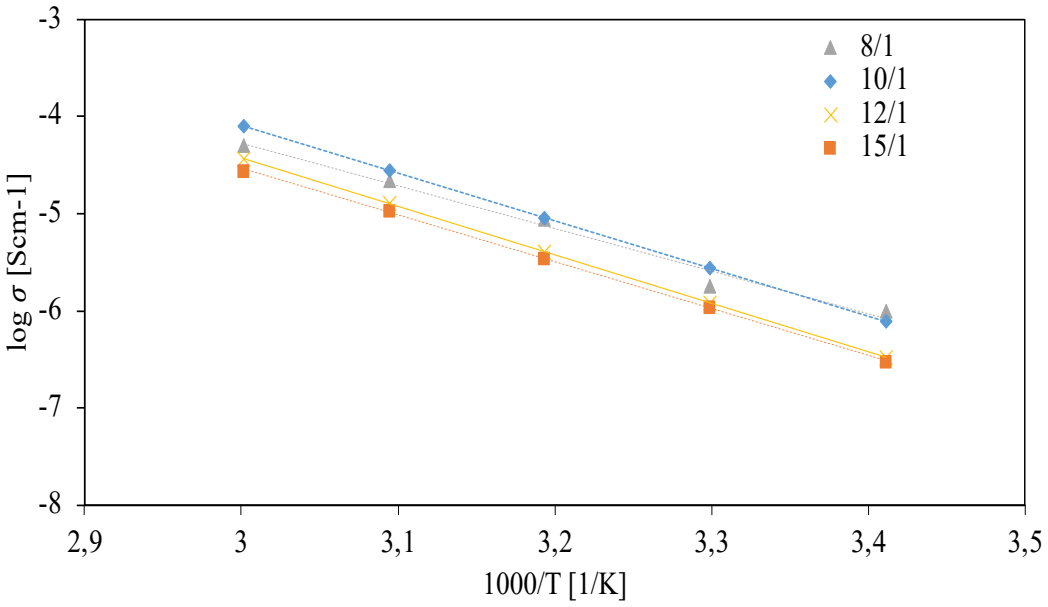

Figure A - 3 Temperature-dependent conductivity of cross-linked G131-based electrolytes without TBP (prepared via Protocol (B)) for different n_{ether}/n_{Li^+} ratios.

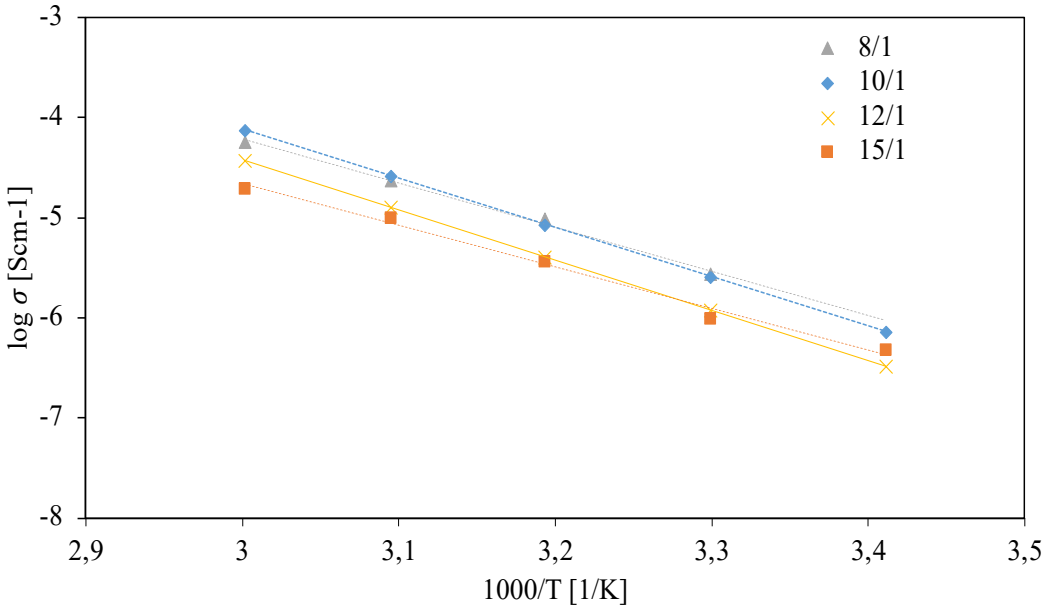

Figure A - 4 Temperature-dependent conductivity of cross-linked G131-based electrolytes with TBP (prepared via Protocol (B)) for different n_{ether}/n_{Li^+} ratios.

REFERENCES

[1] Zubi G, Dufo-López R, Carvalho M, Pasaoglu G. The lithium-ion battery: State of the art and future perspectives. Renewable and Sustainable Energy Reviews. 2018; 89: 292-308.

[2] Helmers E, Marx P. Electric cars: technical characteristics and environmental impacts. Environmental Sciences Europe. 2012; 24(1): 14.

[3] Safari M. Battery electric vehicles: Looking behind to move forward. Energy Policy. 2018; 115: 54-65.

[4] Ornes S. News Feature: The tricky challenge holding back electric cars. Proc Natl Acad Sci U S A. 2021; 118 (26).

[5] Colin McKerracher AOD, Nick Albanese, Dr. Nikolas Soulopoulos. Electric vehicle outlook. BloombergNEF; 2021.

[6] Fan X, Liu B, Liu J, Ding J, Han X, Deng Y, et al. Battery Technologies for Grid-Level Large-Scale Electrical Energy Storage. Transactions of Tianjin University. 2020; 26(2) : 92-103.

[7] Sauer DU. Chapter 2 - Classification of Storage Systems. In: Moseley PT, Garche J, editors. Electrochemical Energy Storage for Renewable Sources and Grid Balancing. Amsterdam: Elsevier; 2015; 13-21.

[8] Strategic Research Agenda for batteries 2020. European Commission; 2020.

[9] Schumm B. Battery. Encyclopedia Britannica. https://www.britannica.com/ technology/battery-electronics. Accessed 15 August 2021.

[10] Park J-K. Principles and Applications of Lithium Secondary Batteries. 1 ed: Wiley-VCH Verlag GmbH & Co. KGaA.

[11] Wong KW, Chow WK. Principle for the Working of the Lithium-Ion Battery. Journal of Modern Physics. 2020; 11(11): 1743-50.

[12] Massé RC, Liu C, Li Y, Mai L, Cao G. Energy storage through intercalation reactions: electrodes for rechargeable batteries. National Science Review. 2016; 4(1): 26-53.

[13] Thompson SE, Parthasarathy S. Moore's law: the future of Si microelectronics. Materials Today. 2006; 9(6): 20-5.

[14] Armand M, Tarascon JM. Building better batteries. Nature. 2008; 451(7179): 652-7.

[15] Vincent CA. Modern Batteries 2nd ed. Vincent CA, Scrosati B, editors. Oxford: Butterworth-Heinemann; 1997; 1-17.

[16] Scrosati B. History of lithium batteries. Journal of Solid State Electrochemistry. 2011; 15(7): 1623-30.

[17] Scharlin P, Battino R. The Voltaic pile: A stimulating general chemistry experiment. Journal of Chemical Education. 1991; 68(8).

[18] Ginsberg J. The Columbia Dry Cell Battery. American Chemical Society, National Historic Chemical Landmarks Program 2005; 3.

[19] Zhu M, Wu J, Wang Y, Song M, Long L, Siyal SH, et al. Recent advances in gel polymer electrolyte for high-performance lithium batteries. Journal of Energy Chemistry. 2019; 37: 126-42.

[20] Takamura T. PRIMARY BATTERIES – AQUEOUS SYSTEMS | Alkaline Manganese–Zinc. In: Garche J, editor. Encyclopedia of Electrochemical Power Sources. Amsterdam: Elsevier; 2009; 28-42.

[21] Whittingham MS. Electrical energy storage and intercalation chemistry. Science. 1976; 192(4244): 1126-7.

[22] Kurzweil P. Gaston Planté and his invention of the lead–acid battery—The genesis of the first practical rechargeable battery. Journal of Power Sources. 2010; 195(14): 4424-34.
[23] Ballantyne A, Hallett J, Riley D, Shah N, Payne D. Lead acid battery recycling for the twenty-first century. Royal Society Open Science. 2018; 5: 13-68.
[24] Beaudin M, Zareipour H, Schellenberglabe A, Rosehart W. Energy Storage for Mitigating the Variability of Renewable Electricity Sources. Energy for Sustainable Development. 2010; 14: 302-14.
[25] Ozcan H, Dincer I. Comprehensive Energy Systems. 2018.
[26] Omar N, Firouz Y, Monem MA, Samba A, Gualous H, Coosemans T, et al. Analysis of Nickel-Based Battery Technologies for Hybrid and Electric Vehicles. Reference Module in Chemistry, Molecular Sciences and Chemical Engineering: Elsevier; 2014.
[27] Koehler U. Electrochemical Power Sources: Fundamentals, Systems, and Applications, Chapter 2 - General Overview of Non-Lithium Battery Systems and their Safety Issues. In: Garche J, Brandt K, editors. Electrochemical Power Sources: Fundamentals, Systems, and Applications: Elsevier; 2019; 21-46.
[28] Kurzweil P, Brandt K. Electrochemical Power Sources: Fundamentals, Systems, and Applications, Chapter 3 - Overview of Rechargeable Lithium Battery Systems. In: Garche J, Brandt K, editors. Electrochemical Power Sources: Fundamentals, Systems, and Applications: Elsevier; 2019; 47-82.
[29] Zhang ZJ, Ramadass P, Fang W. 18 - Safety of Lithium-Ion Batteries. In: Pistoia G, editor. Lithium-Ion Batteries. Amsterdam: Elsevier; 2014; 409-35.
[30] Mekonnen Y, Sundararajan A, Sarwat AI, editors. A review of cathode and anode materials for lithium-ion batteries. SoutheastCon; 2016.
[31] Tarascon JM, Gozdz AS, Schmutz C, Shokoohi F, Warren PC. Performance of Bellcore's plastic rechargeable Li-ion batteries. Solid State Ionics. 1996; 86-88: 49-54.
[32] Nitta N, Wu F, Lee JT, Yushin G. Li-ion battery materials: present and future. Materials Today. 2015; 18(5): 252-64.
[33] Yoshino A. The Birth of the Lithium-Ion Battery. Angewandte Chemie International Edition. 2012; 51(24): 5798-800.
[34] Chapman B. How does a lithium-Ion battery work. 2019; https://letstalkscience.ca/educational-resources/stem-in-context/how-does-a-lithium-ion-battery-work. Accessed 15 August 2021.
[35] Armand M, Axmann P, Bresser D, Copley M, Edström K, Ekberg C, et al. Lithium-ion batteries – Current state of the art and anticipated developments. Journal of Power Sources. 2020; 479.
[36] Mizushima K, Jones PC, Wiseman PJ, Goodenough JB. LixCoO2 (0<x<-1): A new cathode material for batteries of high energy density. Materials Research Bulletin. 1980; 15(6): 783-89.
[37] Hawley WB, Li J. Electrode manufacturing for lithium-ion batteries—Analysis of current and next generation processing. Journal of Energy Storage. 2019; 25.
[38] Zhang M, Mei H, Chang P, Cheng L. 3D printing of structured electrodes for rechargeable batteries. Journal of Materials Chemistry A. 2020; 8(21): 670-94.
[39] Montanino M, Passerini S, Appetecchi G. Electrolytes for rechargeable lithium batteries. Rechargeable Lithium Batteries: From Fundamentals to Applications. 2015: 73-116.
[40] Chombo PV, Laoonual Y. A review of safety strategies of a Li-ion battery. Journal of Power Sources. 2020; 478.

[41] Shin J-H, Henderson WA, Passerini S. Ionic liquids to the rescue? Overcoming the ionic conductivity limitations of polymer electrolytes. Electrochemistry Communications. 2003; 5(12): 1016-20.
[42] Chawla N, Bharti N, Singh S. Recent Advances in Non-Flammable Electrolytes for Safer Lithium-Ion Batteries. Batteries. 2019; 5(1).
[43] Zhou D, Shanmukaraj D, Tkacheva A, Armand M, Wang G. Polymer Electrolytes for Lithium-Based Batteries: Advances and Prospects. Chem. 2019; 5(9): 2326-52.
[44] Nair J, Imholt L, Brunklaus G, Winter M. Lithium Metal Polymer Electrolyte Batteries: Opportunities and Challenges. The Electrochemical Society Interface. 2019; 28:55-61.
[45] Xue Z, He D, Xie X. Poly(ethylene oxide)-based electrolytes for lithium-ion batteries. J Mater Chem A. 2015; 3.
[46] Mindemark J, Lacey MJ, Bowden T, Brandell D. Beyond PEO—Alternative host materials for Li+-conducting solid polymer electrolytes. Progress in Polymer Science. 2018; 81: 114-43.
[47] Hatakeyama-Sato K, Umeki M, Tezuka T, Oyaizu K. Charge-Transfer Complexes for Solid-State Li+ Conduction. ACS Applied Electronic Materials. 2020; 2(7): 2211-7.
[48] Wang L, Li J, Lu G, Li W, Tao Q, Shi C, et al. Fundamentals of Electrolytes for Solid-State Batteries: Challenges and Perspectives. Frontiers in Materials. 2020; 7.
[49] Varzi A, Raccichini R, Passerini S, Scrosati B. Challenges and prospects of the role of solid electrolytes in the revitalization of lithium metal batteries. Journal of Materials Chemistry. 2016; 4: 17251-9.
[50] Cao C, Li Z-B, Wang X-L, Zhao X-B, Han W-Q. Recent Advances in Inorganic Solid Electrolytes for Lithium Batteries. Frontiers in Energy Research. 2014; 2(25).
[51] Famprikis T, Canepa P, Dawson JA, Islam MS, Masquelier C. Fundamentals of inorganic solid-state electrolytes for batteries. Nat Mater. 2019; 18(12): 1278-91.
[52] Ashby MF. Chapter 11 - Designing Hybrid Materials. In: Ashby MF, editor. Materials Selection in Mechanical Design (Fourth Edition). Oxford: Butterworth-Heinemann; 2011; 299-340.
[53] Li S, Zhang S-Q, Shen L, Liu Q, Ma J-B, Lv W, et al. Progress and Perspective of Ceramic/Polymer Composite Solid Electrolytes for Lithium Batteries. Advanced Science. 2020;7(5): 1903088.
[54] Yao P, Yu H, Ding Z, Liu Y, Lu J, Lavorgna M, et al. Review on Polymer-Based Composite Electrolytes for Lithium Batteries. Front Chem. 2019; 7: 522.
[55] Liu X, Li X, Li H, Wu HB. Recent Progress of Hybrid Solid-State Electrolytes for Lithium Batteries. Chemistry. 2018; 24(69): 18293-306.
[56] Arora P, Zhang Z. Battery Separators. Chemical Reviews. 2004; 104(10): 4419-62.
[57] Denissen W, Winne JM, Du Prez FE. Vitrimers: permanent organic networks with glass-like fluidity. Chem Sci. 2016; 7(1): 30-8.
[58] Guerre M, Taplan C, Winne JM, Du Prez FE. Vitrimers: directing chemical reactivity to control material properties. Chem Sci. 2020; 11(19): 4855-70.
[59] Li T, Zhang ZP, Rong MZ, Zhang MQ. Self-healable and thiol–ene UV-curable waterborne polyurethane for anticorrosion coating. Journal of Applied Polymer Science. 2019; 136(26).
[60] Lei ZQ, Xiang HP, Yuan YJ, Rong MZ, Zhang MQ. Room-Temperature Self-Healable and Remoldable Cross-linked Polymer Based on the Dynamic Exchange of Disulfide Bonds. Chemistry of Materials. 2014; 26(6): 2038-46.
[61] Kalhoff J, Eshetu G, Bresser D, Passerini S. Safer Electrolytes for Lithium-Ion Batteries: State of the Art and Perspectives. ChemSusChem. 2015; 8: 2154-75.

[62] Chen D, Wang D, Yang Y, Huang Q, Zhu S, Zheng Z. Self-Healing Materials for Next-Generation Energy Harvesting and Storage Devices. Advanced Energy Materials. 2017; 7(23): 1700890.
[63] Zhou B, He D, Hu J, Ye Y, Peng H, Zhou X, et al. A flexible, self-healing and highly stretchable polymer electrolyte via quadruple hydrogen bonding for lithium-ion batteries. Journal of Materials Chemistry A. 2018; 6(25): 11725-33.
[64] ThioplastTM G SH-functionalized telechelic polymers https://sulfurderivatives.nouryon.com/thioplast/: Nouryon Functional Chemicals GmbH; 2021. Accessed 15 August 2021.
[65] Astruc D. The metathesis reactions: from a historical perspective to recent developments. New Journal of Chemistry. 2005; 29(1): 42-56.
[66] Nevejans S, Ballard N, Miranda J, Reck B, Asua J. The underlying mechanisms for self-healing of poly(disulfide)s. Phys Chem Chem Phys. 2016; 18.
[67] Boujioui, Gohy. Ion-Conducting Redox-Active Polymer Gels Based on Stable Nitroxide Radicals. Polymers. 2019; 11: 1322.
[68] Xiamen Tmax Battery Equipments Limited. https://www.batterymaking.com/product/316-stainless-steel-cr2032-2025-2016-coin-cell-case-with-o-rings_p172.html. Accessed 15 August 2021.

UNIVERSITÉ CATHOLIQUE DE LOUVAIN
École polytechnique de Louvain
Rue Archimède, 1 bte L6.11.01, 1348 Louvain-la-Neuve, Belgique | **www.uclouvain.be/epl**